

**Electronic Supplementary Information
for**

Right- and left-handed PPI helices in cyclic dodecapeptoids

Giovanni Pierri, Rosaria Schettini, Francesco F. Summa, Francesco De Riccardis, Guglielmo Monaco, Irene Izzo* and Consiglia Tedesco*

Department of Chemistry and Biology “A. Zambelli”, University of Salerno, Via Giovanni Paolo II 132, 84084 Fisciano (SA), Italy.

*to whom correspondence should be addressed: iizzo@unisa.it, ctedesco@unisa.it

TABLE OF CONTENTS

1.0 List of abbreviations	S3
2.0 Synthesis.....	S4
2.1 General procedures.....	S4
2.2 Synthesis of the linear precursors of 2-4.....	S4
2.3 General procedure for the high dilution cyclization: synthesis of 2-4	S6
3.0 RP-HPLC of linear precursors of cyclic peptoids 2-4.....	S9
4.0 RP-HPLC, ¹H- and ¹³C NMR spectra of cyclic peptoids 2-4	S12
5.0 X-ray crystallography	S18
5.1 Single crystal X-ray diffraction	S18
5.2 Intramolecular interactions	S24
5.2.1 CO···CO interactions	S24
5.2.2 Backbone CH···OC hydrogen bonds	S27
5.2.3 Intramolecular C5 CH···OC interactions.....	S29
5.2.4 Intramolecular C6 CH···HC contacts.....	S31
5.2.5 Intramolecular C6 CH···OC interactions.....	S33
5.2.6 Intramolecular C7 CH···OC interactions.....	S34
5.3 Crystal packing	S36
6.0 Quantum Mechanical Computations	S40
6.1 Interactions energies: Espinosa-Molins-Lecomte equation	S40
6.2 Non-Covalent Interactions Analysis.....	S43
6.3 Cartesian coordinates of fully optimized 1 at the B3LYP/6-311G(d,p) level	S45
6.4 Cartesian coordinates of fully optimized 1 at the B3LYP/6-311+G(d,p) level	S47
7.0 References	S51

1.0 List of abbreviations

ACN: acetonitrile

DCM: dichloromethane

DIC: *N,N'*-diisopropylcarbodiimide

DIPEA: *N,N*-diisopropylethylamine

DMF: *N,N*-dimethylformamide

HFIP: 1,1,1,3,3,3-hexafluoro-2-propanol

HATU: *O*-(7-azabenzotriazol-1-yl)-*N,N,N',N'*-tetramethyluronium hexafluorophosphate

RP-HPLC: reversed-phase high-performance liquid chromatography

TFA: trifluoroacetic acid

2.0 Synthesis

2.1 General procedures

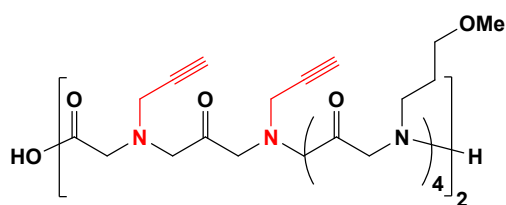
Starting materials and reagents purchased from commercial suppliers were generally used without purification unless otherwise mentioned. Reactions were monitored by analytical thin layer chromatography (TLC) on precoated silica gel plates (0.25 mm) and visualized by UV light. The purity grade of cyclic peptoids were checked by HPLC analysis using a C18 reversed-phase analytical column (Bondapak, 10 μ m, 125 \AA , 3.9 mm \times 300 mm) run with linear gradients of ACN (0.1% TFA) into H₂O (0.1% TFA) over 30 min, at a flow rate of 1.0 mL/min, using a Modular HPLC System JASCOLC-NET II/ADC equipped with a JASCO Model PU-2089 PlusPump and a JASCO MD-2010 Plus UV-vis multiple wavelength detector set at 220 nm. High resolution mass spectra (HRMS) were recorded on a Bruker Solarix XR Fourier transform ion cyclotron resonance mass spectrometer (FTICR-MS) equipped with a 7T magnet, using matrix-assisted laser desorption/ionization (MALDI). Yields refer to chromatographically and/or spectroscopically (¹H- and ¹³C NMR) pure materials. ¹H NMR and ¹³C spectra were recorded on Bruker DRX 600 (1H at 600.13 MHz, 13C at 150.90 MHz) and Bruker DRX 400 (1H at 400.13 MHz, 13C at 100.03 MHz). Chemical shifts (δ) are reported in ppm relative to the residual solvent peak (CHCl₃, δ = 7.26; ¹³CDCl₃, δ = 77.0) and the multiplicity of each signal is designated by the following abbreviations: s, singlet; d, doublet; t, triplet; m, multiplet; bs, broad singlet; bd, broad doublet. Coupling constants (J) are quoted in Hertz.

2.2 Synthesis of the linear precursors of 2-4.

2-chlorotriyl chloride resin (2, α -dichlorobenzhydryl-polystyrene cross-linked with 1% DVB; 100–200 mesh; 1.63 mmol g⁻¹, 0.400 g, 0.652 mmol) was washed with DCM (3 \times 2 mL) and DMF (3 \times 2 mL) and then swelled in dry DCM (2 mL) for 45 min. Bromoacetic acid (0.145 g, 1.04 mmol) and DIPEA (0.600 mL, 3.26 mmol) in dry DCM (2 mL) were added to the resin and the vessel was stirred on a shaker platform for 60 min at room temperature. After the resin was washed with DMF (3 \times 2 mL), DCM (3 \times 2 mL) and then with DMF (3 \times 2 mL), a solution of propargyl amine (0.42 mL, 6.52 mmol) in dry DMF (2 mL) was added to the bromoacetylated resin. The mixture was left on the shaker platform for 40 min at room temperature, and then the resin was washed with DMF (3 \times 2 mL), DCM (3 \times 2 mL) and then with DMF (3 \times 2 mL). Subsequent bromoacetylation reaction was accomplished by reacting the oligomer with a solution of bromoacetic acid (0.906 g, 6.52 mmol) and DIC (1.11 mL, 7.17 mmol) in dry DMF (2 mL), stirring on a shaker platform for 40 min at room temperature. Then the reaction with the proper amine (propargyl amine (0.42 mL, 6.52 mmol) or (methoxyethyl amine (0.57 mL, 6.52 mmol)) was realized as described above. The synthesis

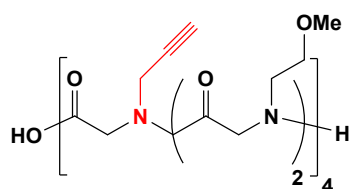
proceeded until the linear target was obtained. The oligomer-resin was cleaved by treatment with three aliquots of a solution of 20% HFIP in dry DCM (v/v; 3×2 mL), with stirring each time on the shaker platform for 30 min at room temperature and filtering the resin away after each treatment. The combined filtrates were concentrated in vacuo. The final product was analyzed by MALDI mass spectrometry and RP-HPLC and used for the cyclization step without further purification.

Linear precursor of 2



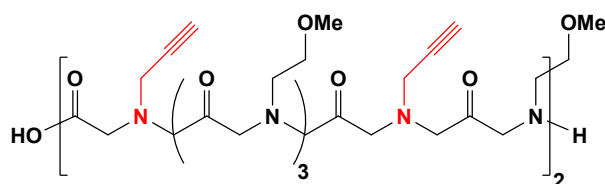
856 mg, >98 % yield, white amorphous solid; RP-HPLC analysis: Bondapak, 5% B in A → 100% B in 30 min (A: 0.1% TFA in water, B: 0.1% TFA in acetonitrile), 1.0 mL/min, 220 nm, t_r 11.2 min.; MS (MALDI) $[M + H]^+$ 1319.9.

Linear precursor of 3



850 mg, >98 % yield, white amorphous solid; RP-HPLC analysis: Bondapak, 5% B in A → 100% B in 30 min (A: 0.1% TFA in water, B: 0.1% TFA in acetonitrile), 1.0 mL/min, 220 nm, t_r 11.0 min.; MS (MALDI) $[M + H]^+$ 1319.7.

Linear precursor of 4

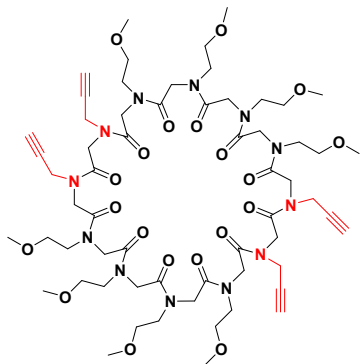


738 mg, 85% yield, white amorphous solid; RP-HPLC analysis: Bondapak, 5% B in A → 100% B in 30 min (A: 0.1% TFA in water, B: 0.1% TFA in acetonitrile), 1.0 mL/min, 220 nm, t_r 11.2 min.; MS (MALDI) $[M + H]^+$ 1319.7.

2.3 General procedure for the high dilution cyclization: synthesis of 2-4

To a stirred solution of HATU (1.062 g, 2.80 mmol) and DIPEA (760 μ L, 4.34 mmol) in dry DMF (210 mL) at room temperature, a solution of the linear precursor (0.70 mmol) in dry DMF (20 mL) was added using a syringe pump in 3 h. After 18 h the resulting mixture was concentrated in vacuo, diluted with DCM (100 mL) and washed with 1 M HCl (2×50 mL). The aqueous layer was extracted with DCM (2×100 mL) and the combined organic phases were washed with water (150 mL), dried over $MgSO_4$ and concentrated in vacuo. The crude cyclic peptoids was flash chromatographed (silica gel, from 10% ethyl acetate in petroleum ether to 50% methanol in ethyl acetate) to give cyclic product as an amorphous solid.

Cyclododecapeptoid 2



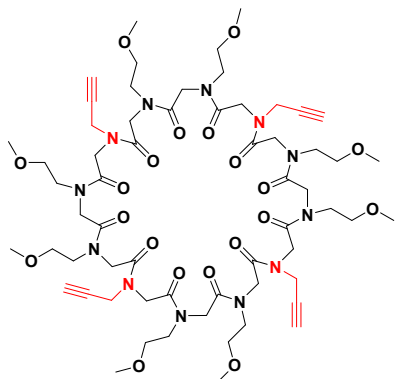
2: 230 mg, 25% yield, white amorphous solid, m.p. 104-105 °C; RP-HPLC analysis: Bondapak, 5% B in A → 100% B in 30 min (A: 0.1% TFA in water, B: 0.1% TFA in acetonitrile), 1.0 mL/min, 220 nm, t_r 13.0 min.;

¹H-NMR: (400 MHz, $CDCl_3$, mixture of rotamers) δ : 4.42-3.95 (m, 32 H, $NCHHCO$, $NCH\underline{H}CO$, NCH_2CCH), 3.38-3.14 (m, 56 H, $NCH_2CH_2OCH_3$, $NCH_2\underline{CH}_2OCH_3$, $NCH_2CH_2OCH_3$), 2.33-2.23 (m, 4 H, NCH_2CCH);

¹³C-NMR: (100 MHz, $CDCl_3$, mixture of rotamers) δ : 169.7, 169.4, 169.1, 168.9, 168.7, 168.7, 168.5, 168.4, 168.2, 168.0, 167.8, 167.6, 78.4, 78.4, 78.3, 78.2, 78.1, 78.1, 78.0, 77.9, 77.8, 73.8, 73.7, 73.5, 73.4, 73.2, 72.8, 72.5, 71.6, 71.3, 71.1, 71.0, 69.8, 69.6, 58.8 (X 2), 58.8 (X 2), 58.4 (X 2), 58.2, 50.2, 49.9, 49.8, 49.7, 49.5, 48.8, 47.9, 47.7, 47.4, 47.2, 47.1, 46.9, 38.1, 37.8, 37.4, 37.3, 37.1, 36.2, 36.0, 35.9.

HRMS (MALDI) [M + H]⁺ calcd for C₆₀H₉₃N₁₂O₂₀, 1301.6624, found 1301.6603.

Cyclododecapeptoid 3



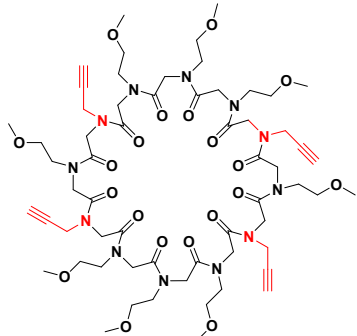
3: 217 mg, 24% yield, white amorphous solid, m.p. 107-108 °C; RP-HPLC analysis: Bondapak, 5% B in A → 100% B in 30 min (A: 0.1% TFA in water, B: 0.1% TFA in acetonitrile), 1.0 mL/min, 220 nm, t_r 12.8 min.;

¹H-NMR: (400 MHz, CDCl₃, mixture of rotamers) δ: 4.38-3.97 (m, 32 H, NCHHCO, NCHHCO, NCH₂CCH), 3.40-3.02 (m, 56 H, NCH₂CH₂OCH₃, NCH₂CH₂OCH₃, NCH₂CH₂OCH₃), 2.34-2.19 (m, 4 H, NCH₂CCH);

¹³C-NMR: (100 MHz, CDCl₃, mixture of rotamers) δ: 169.8, 169.6, 169.4, 169.3, 169.1, 169.0, 168.9, 168.8, 168.7, 168.6, 168.6, 168.4, 168.2, 168.2, 167.7, 167.6, 167.5, 78.6, 78.5, 78.4, 78.4, 73.6, 73.4, 73.2, 72.9, 72.6, 72.5, 72.3, 71.6, 71.5, 71.1, 71.0, 70.8, 70.1, 70.0, 69.7, 69.5, 58.8 (x 2), 58.5 (x 2), 58.5 (x 2), 58.3, 58.2, 50.3, 50.1, 49.9, 49.7, 48.5, 47.8, 47.7, 47.5, 47.2, 47.1, 46.2, 38.1, 37.9, 37.8, 37.6, 37.4, 37.1, 36.5, 36.2, 36.0, 35.9.

HRMS (MALDI) [M + H]⁺ calcd for C₆₀H₉₃N₁₂O₂₀ 1301.6624, found 1301.6610.

Cyclododecapeptoid 4



236 mg, 36% yield, white amorphous solid, m.p. 75-76 °C; RP-HPLC analysis: Bondapak, 5% B in A → 100% B in 30 min (A: 0.1% TFA in water, B: 0.1% TFA in acetonitrile), 1.0 mL/min, 220 nm, t_r 13.0 min.;

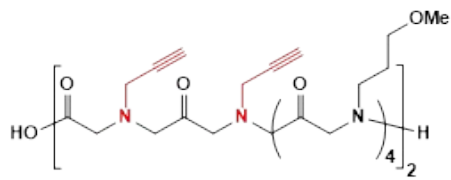
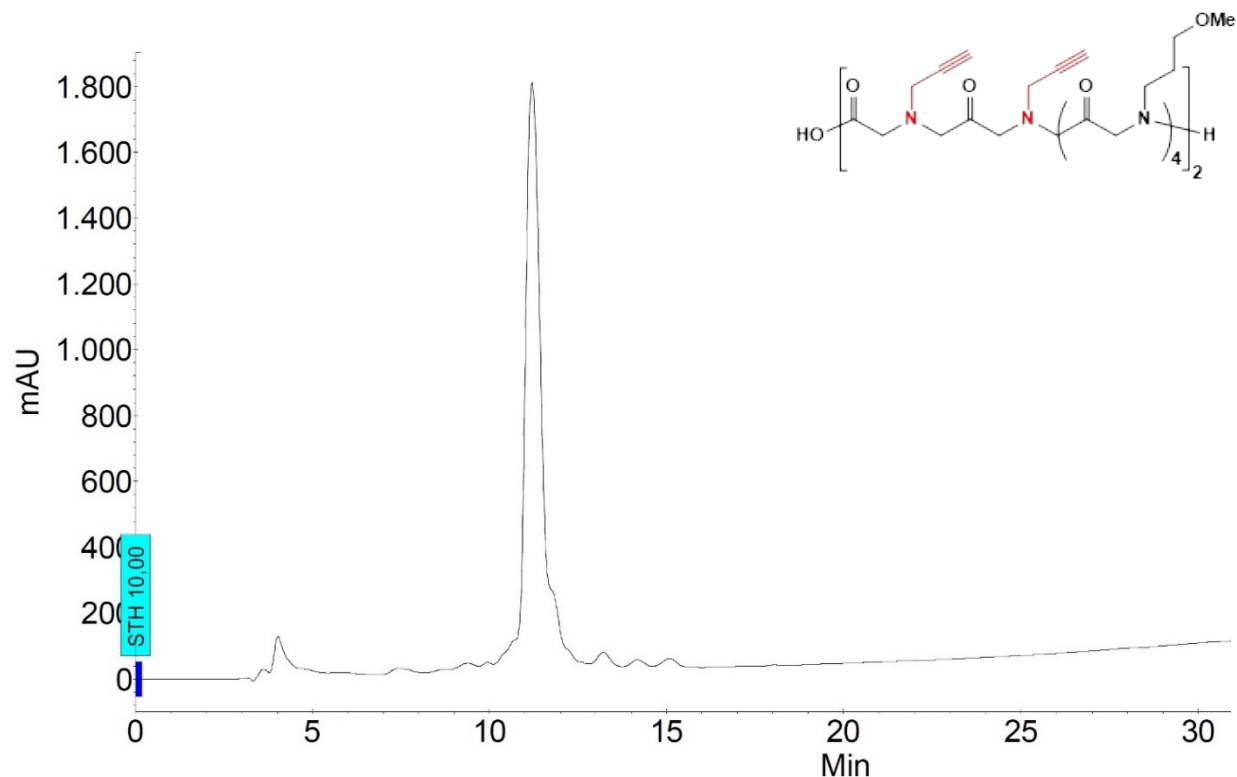
¹H-NMR: (400 MHz, CDCl₃, mixture of rotamers) δ: 4.39-4.04 (m, 32 H, NCHHCO, NCHHCO, NCH₂CCH), 3.43-3.22 (m, 56 H, NCH₂CH₂OCH₃, NCH₂CH₂OCH₃, NCH₂CH₂OCH₃), 2.35-2.06 (m, 4 H, NCH₂CCH);

¹³C-NMR: (100 MHz, CDCl₃, mixture of rotamers) δ: 170.0, 169.8, 169.7, 169.5, 169.4, 169.3, 169.2, 69.0, 168.8, 168.7, 168.6, 168.4, 168.3, 168.1, 78.5, 78.4, 78.3, 78.1, 73.9, 73.7, 73.4, 73.3, 73.0, 72.8, 72.6, 72.5, 71.7, 71.6, 71.2, 71.1, 70.9, 69.8, 69.6, 69.5, 58.9 (X 2), 58.8(X 2), 58.6 (X 2), 58.5 (X 2), 58.4, 50.5, 50.2, 49.9, 49.8, 49.1, 48.8, 48.5, 48.4, 48.0, 47.3, 47.0, 38.1, 37.6, 37.3, 36.9, 36.6, 36.2, 36.1.

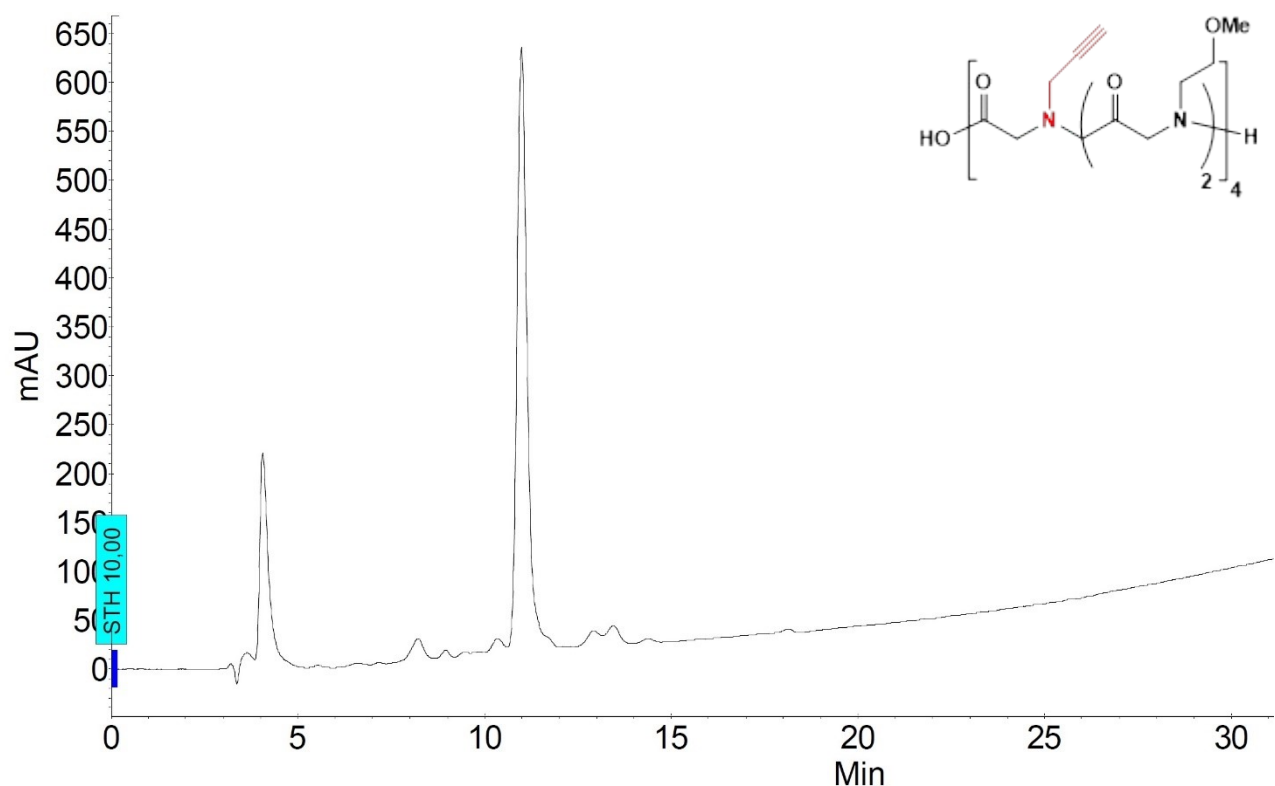
HRMS (MALDI) [M + H]⁺ calcd for C₆₀H₉₃N₁₂O₂₀ 1301.6624, found 1301.6691.

3.0 RP-HPLC of linear precursors of cyclic peptoids 2-4

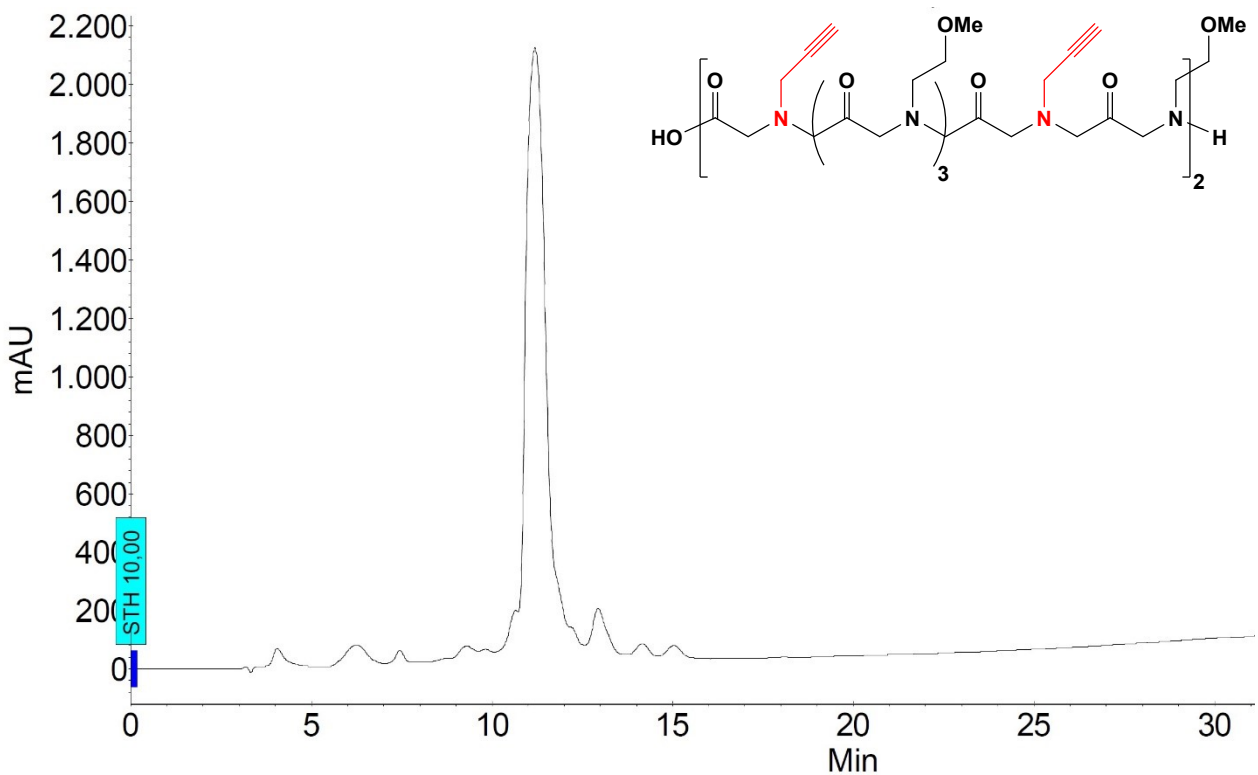
RP-HPLC of linear precursor of 2



RP-HPLC of linear precursor of 3

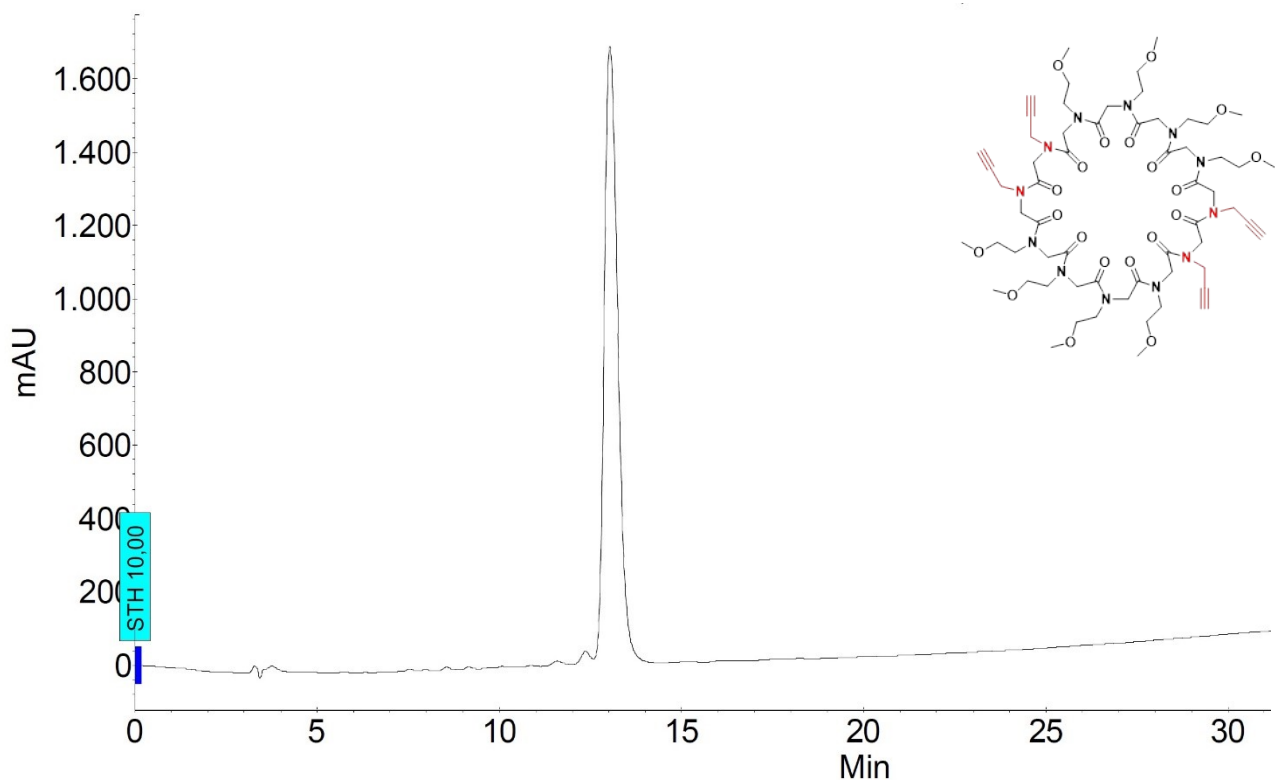


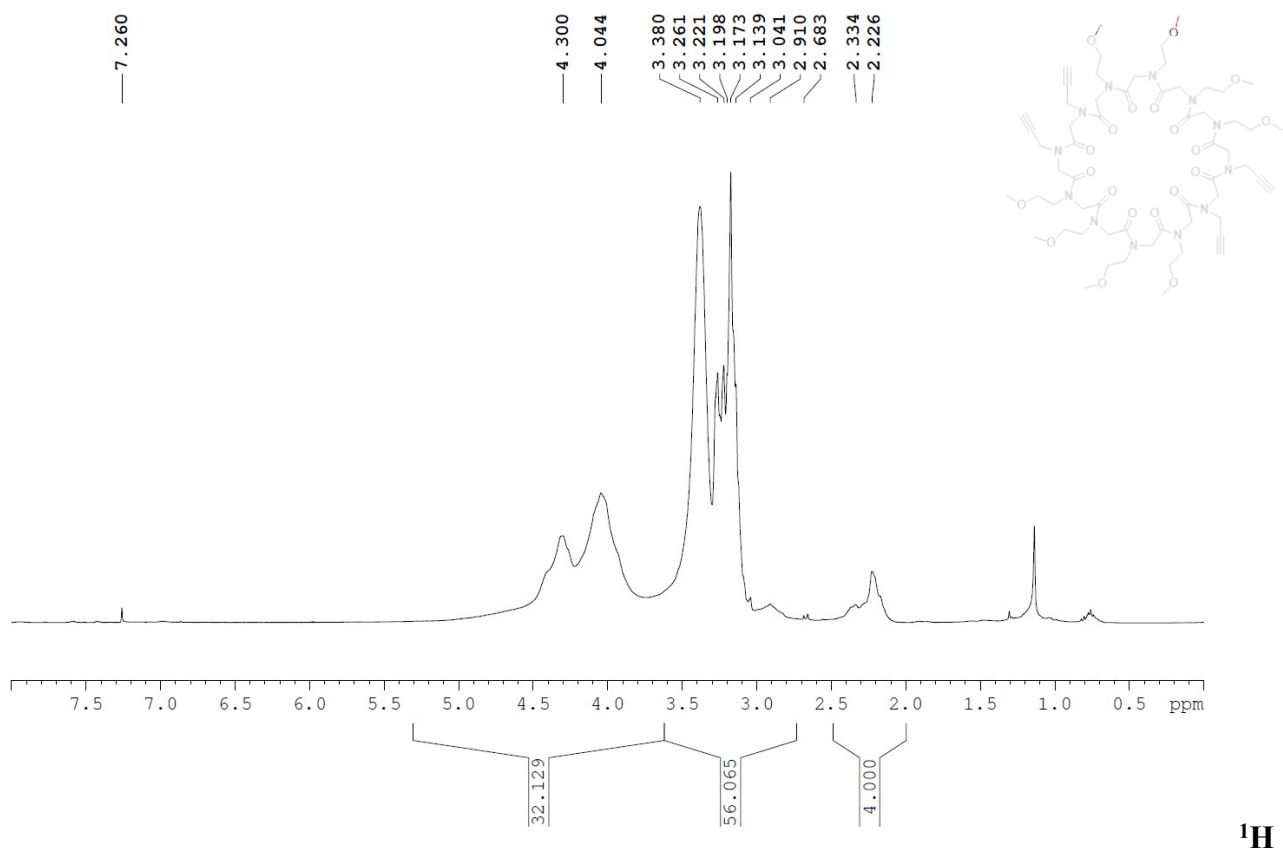
RP-HPLC of linear precursor of 4



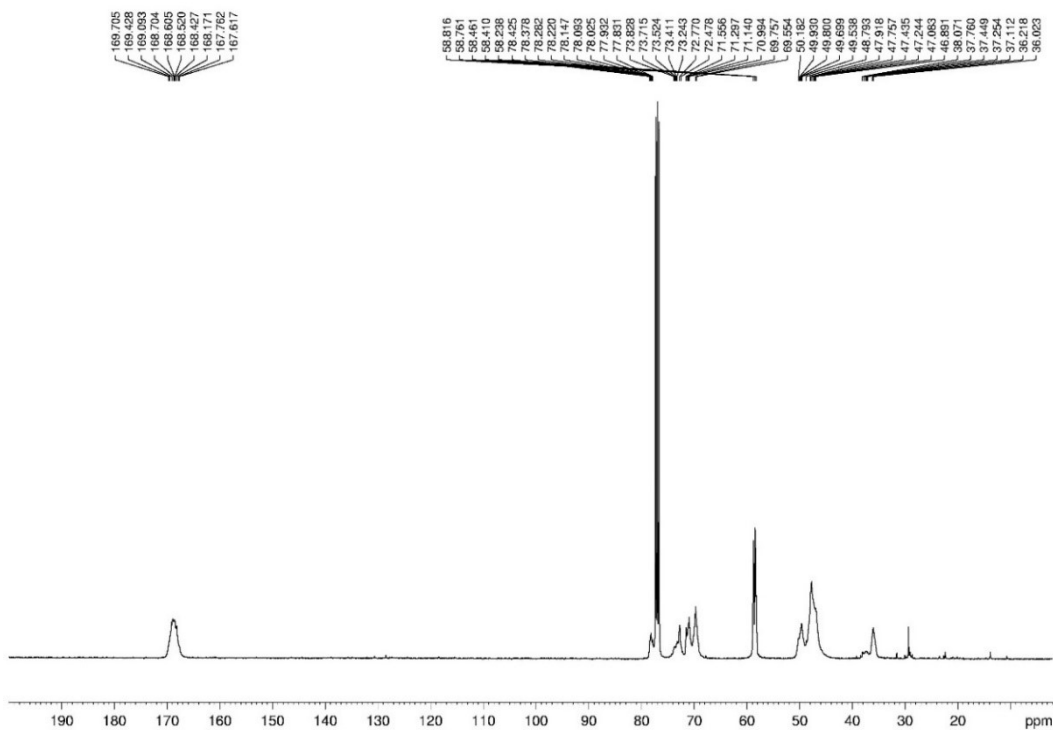
4.0 RP-HPLC, ^1H - and ^{13}C NMR spectra of cyclic peptoids 2-4

RP-HPLC of compound 2



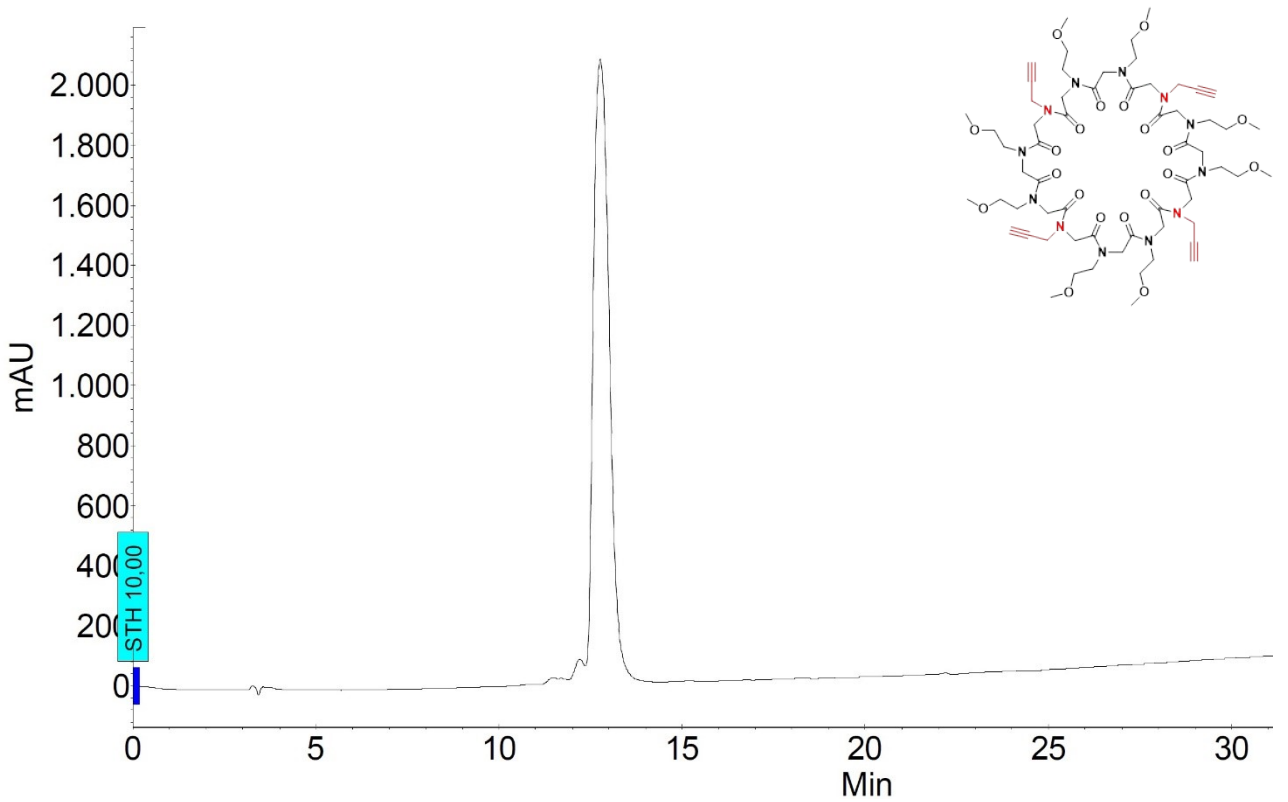


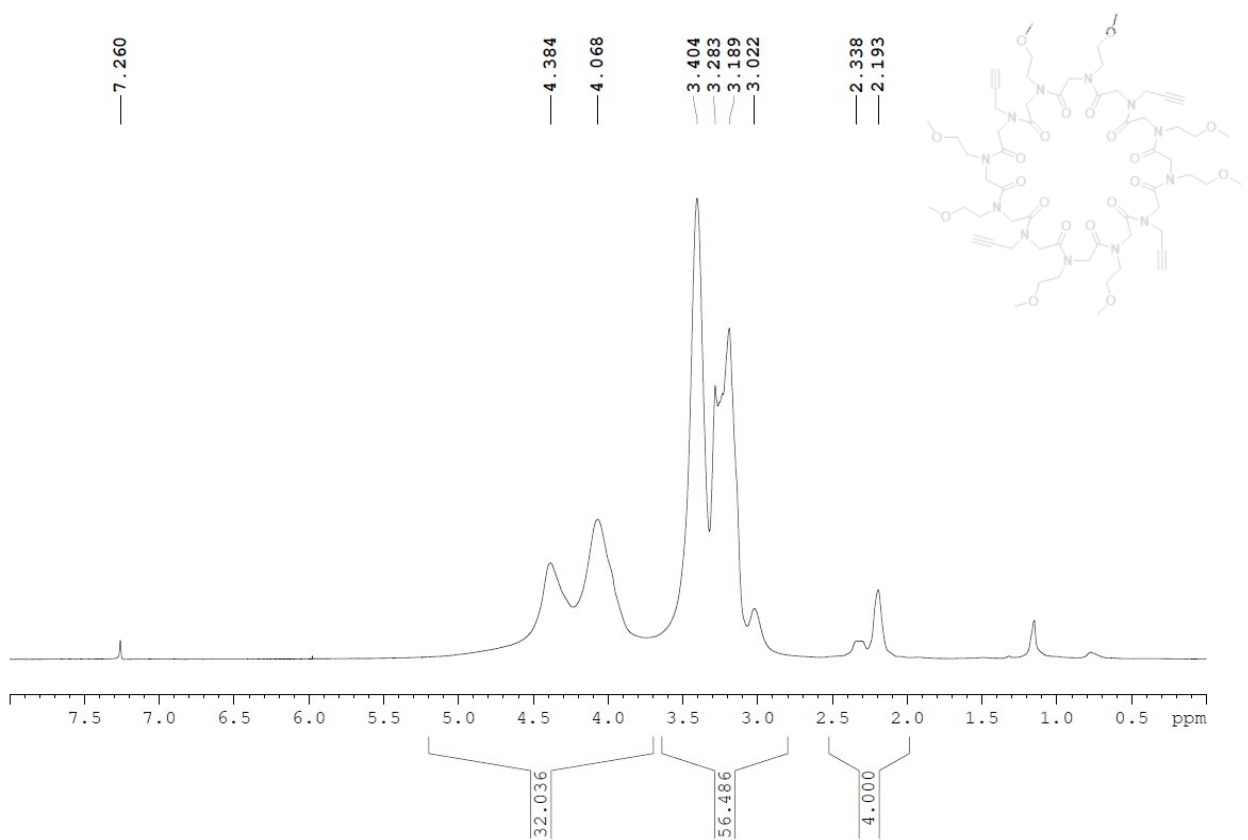
-NMR of compound 2 (400 MHz, CDCl₃)



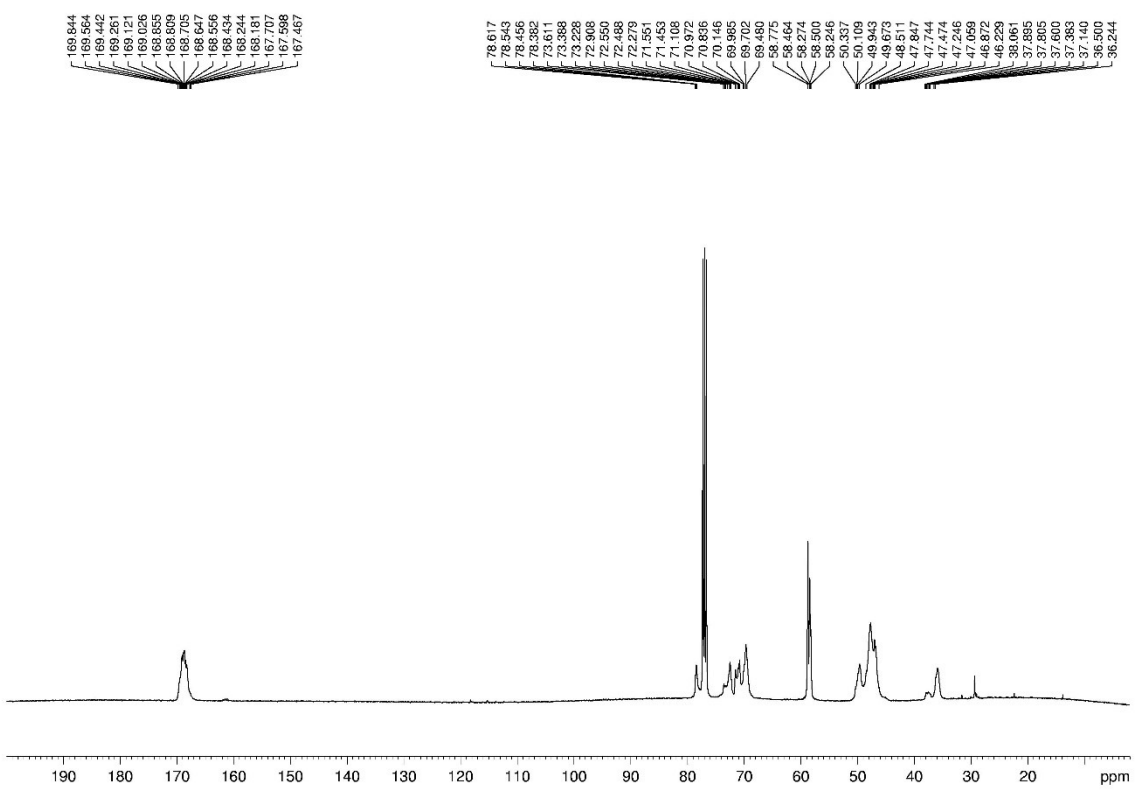
¹³C-NMR of compound 2 (100 MHz, CDCl₃)

RP-HPLC of compound 3

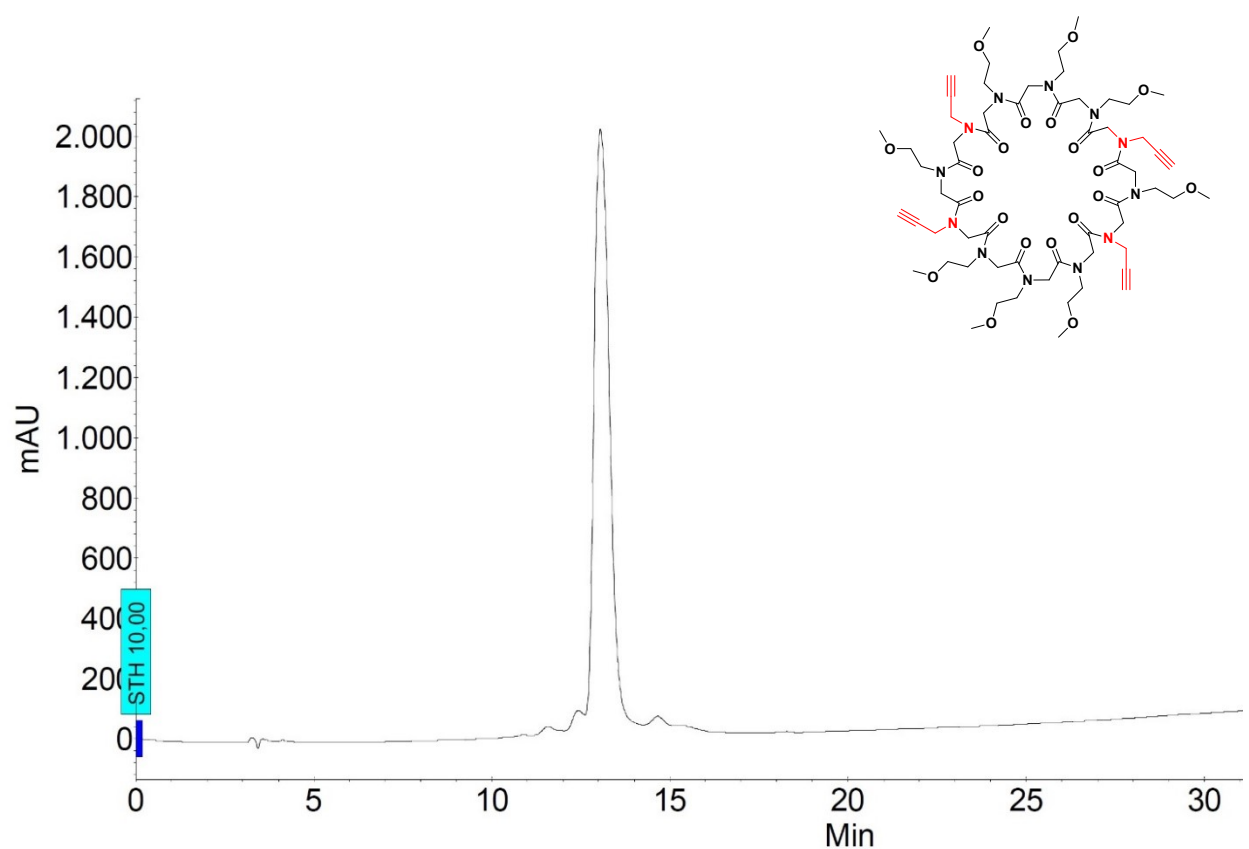


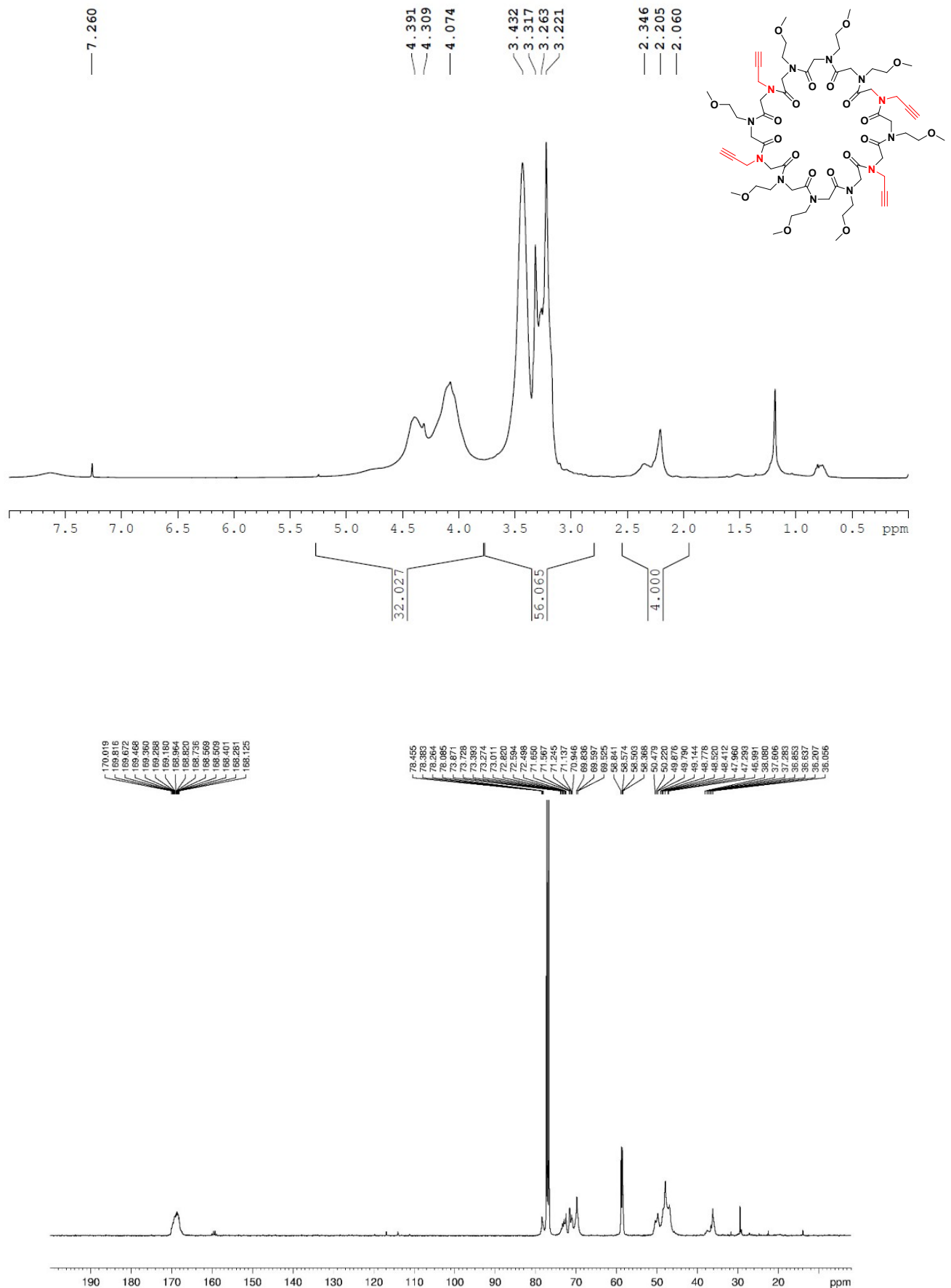


¹H-NMR of compound 3 (400 MHz, CDCl₃)



RP-HPLC of compound 4





¹H-NMR of compound 4 (400 MHz, CDCl₃)

¹³C-NMR of compound 4 (100 MHz, CDCl₃)

5.0 X-ray crystallography

5.1 Single crystal X-ray diffraction

Crystals of compound **1** suitable for single crystal X-ray diffraction analysis were obtained by slow evaporation, dissolving 5 mg of the compound in methanol and then adding toluene reaching a final ratio of 2:1. For the measurement, a colourless prismatic crystal of 0.54 mm x 0.33 mm x 0.15 mm was selected.

Crystals of the compound **2** suitable for single crystal X-ray diffraction analysis were obtained by slow evaporation, dissolving 5 mg of the compound in ethyl acetate and then adding toluene reaching a final ratio of 1:1. For the measurement, a colourless prismatic crystal of 0.37 mm x 0.24 mm x 0.09 mm was selected.

Crystals of the compound **3** suitable for single crystal X-ray diffraction analysis were obtained by slow evaporation, dissolving 5 mg of the compound in isopropyl alcohol. For the measurement, a colourless prismatic crystal of 0.59 mm x 0.19 mm x 0.07 mm was selected.

Crystals of the compound **4** suitable for single crystal X-ray diffraction analysis were obtained by slow evaporation, dissolving 5 mg of the compound in chloroform, and then adding diethyl ether reaching a final ratio of 1:2. For the measurement, a colourless prismatic crystal of 0.53 mm x 0.31 mm x 0.11 mm was selected.

To avoid the loss of guest molecules of compounds **1**, **2** and **3**, the crystals were inserted in glass capillaries and sealed. As for compound **4**, crystals were mounted on a cryoloop with paratone oil.

All the data collections were performed at room temperature with a Bruker D8 QUEST diffractometer equipped with a PHOTON II detector using CuK α radiation ($\lambda = 1.54178 \text{ \AA}$).

Data Indexing were performed using APEX3.¹ Data integration and reduction were performed using SAINT.¹ Absorption correction were performed by multi-scan method in SADABS.¹ The structures were solved using SHELXS-97² and refined through full matrix least-squares based on F^2 using the program SHELXL.³

ORTEP diagrams (Figure S1) were drawn using OLEX2.⁴ In Table S1 are reported the crystallographic data.

Compound **1** crystallizes as a methanol/toluene solvate form. At first we tried to model the disordered guest molecules, which occupy two different sites. In the first site a methanol molecule with an

occupancy factor of 0.782(9) is localized, in the second one both toluene and methanol molecules are localized. In the latter case, a free variable was used to refine their occupancy factors by constraining the sum of the two values to 0.75 and obtaining final occupancy factors of 0.412(9) and 0.338(9) for toluene and methanol, respectively. Following reviewer's suggestion, we decided to mask the solvent. A solvent mask was calculated, and 132 electrons were found in a volume of 740 Å³ in 1 void per unit cell. Using the occupancy factors obtained in the first structure model, we obtained that in this void should be present about 1.1 CH₄O and 0.4 C₇H₈ molecules, which account for 116 electrons per unit cell.

The *cis* propargyl side chain attached to the nitrogen atom N2 shows positional disorder with a refined occupancy of 0.69(4) and 0.31(4).

Compound **2** crystallizes as an ethyl acetate solvate. Also in this case, a starting model including the guest molecule was refined with the ethyl acetate molecules localized between host columns with full occupancy. Then, following reviewer's suggestion, we decided to mask the guest molecule. A solvent mask was calculated and 188 electrons were found in a volume of 700 Å³ in 1 void per unit cell. This is consistent with the presence of 2 ethyl acetate molecules per formula unit which account for 192 electrons per unit cell.

The oxygen atom O7A (belonging to the methoxyethyl side chain attached to nitrogen atom N1) shows positional disorder occupying two possible positions with a refined occupancy of 0.845(15) and 0.155(15).

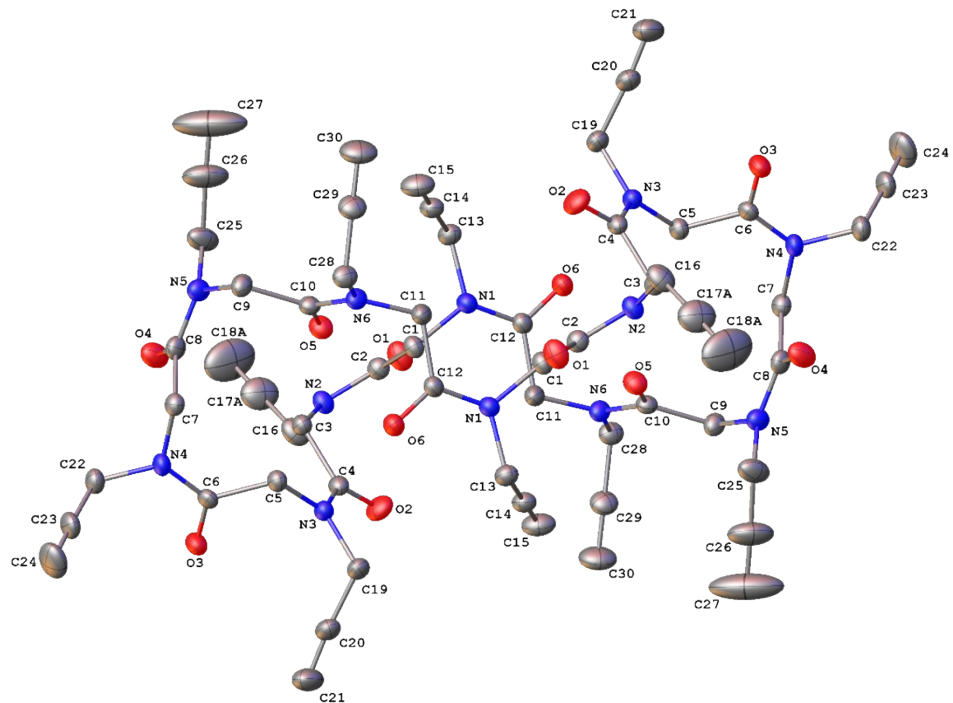
Compound **3** crystallizes as an isopropanol solvate. The starting model shows isopropanol molecules disordered over two possible positions with a refined occupancy of 0.575(11) and 0.425(11). Moreover, a water molecule (O1W) is present too with a refined occupancy factor of 0.278(6). As for crystal structures of compound **1** and **2**, following reviewer's suggestion, the disordered isopropanol molecules were masked. A solvent mask was calculated and 65 electrons were found in a volume of 321 Å³ in 1 void per unit cell. This is consistent with the presence of 2 isopropanol molecules per formula unit which account for 68 electrons per unit cell.

The *cis* methoxyethyl side chain attached to the nitrogen atom N2 is disordered over two positions with refined occupancy of 0.510(7) and 0.490(7). The *cis* methoxyethyl side chain attached to the nitrogen atom N3 shows positional disorder for the carbon atom C20A and C20B with a final refined occupancy of 0.586(11) and 0.414(11).

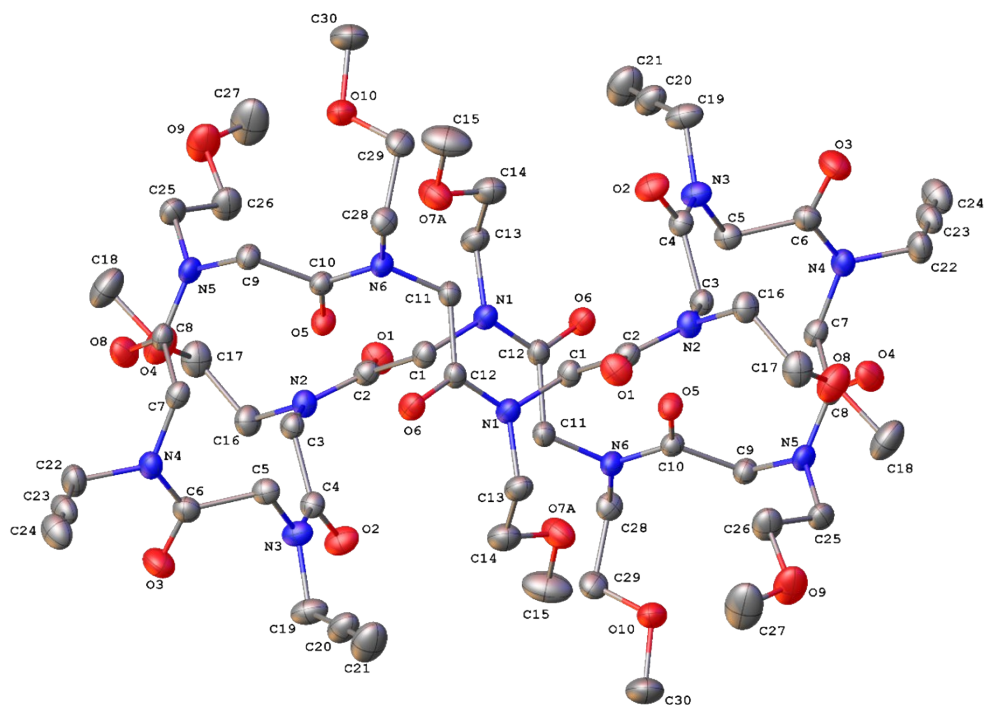
Compound **4** shows disorder on the two *cis* methoxyethyl side chains. In particular, the disordered atoms of the side chain attached to the nitrogen atom N1 can occupy two different positions with

refined occupancy of 0.594(14) and 0.406(14), while the disordered atoms attached to the nitrogen atom N4 show a refined occupancy factor of 0.569(17) and 0.407(14).

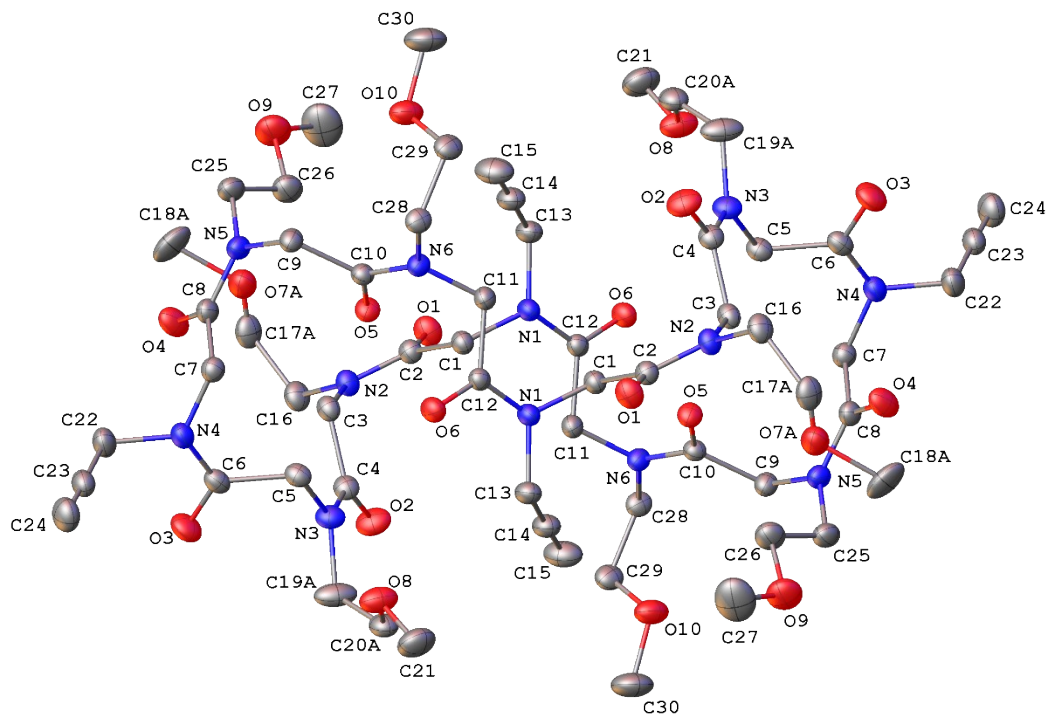
For all the crystal structures, non-hydrogen atoms were refined anisotropically, hydrogen atoms were positioned geometrically and included in structure factors calculations but not refined. Some restraints were used for the water molecule hydrogen atoms in crystal structure of compound **3**.



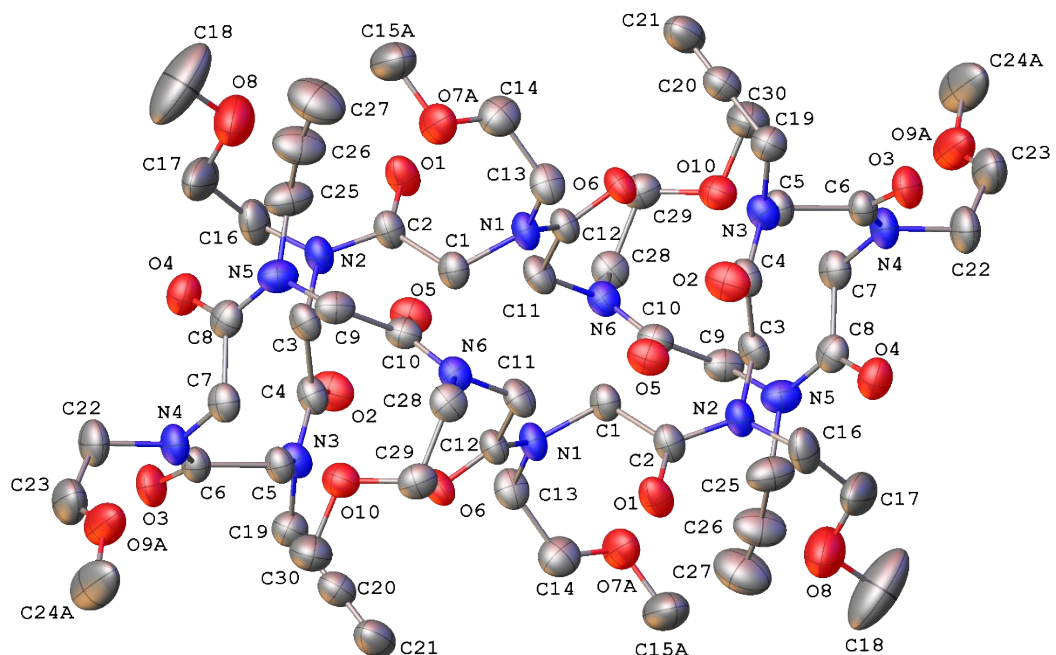
(a)



(b)



(c)



(d)

Figure S1. ORTEP drawings for crystal structures of compound 1 (a); compound 2 (b), compound 3 (c) and compound 4 (d). Atom types: C grey, O red, N blue. Hydrogen atoms and water molecule in crystal structure of 3 are omitted for clarity. For clarity, only the atoms with the highest occupancy factor are shown. Ellipsoids are drawn at 20% probability level.

Table S1. Crystallographic data for compounds **1**, **2**, **3** and **4**.

	1	2	3	4
T (K)	296	296	296	296
Formula	C ₆₀ H ₆₀ N ₁₂ O ₁₂ 0.412(C ₇ H ₈) 2.24(CH ₃ OH)	C ₆₀ H ₉₂ N ₁₂ O ₂₀ 2(C ₄ H ₈ O ₂)	C ₆₀ H ₉₂ N ₁₂ O ₂₀ 2(C ₃ H ₈ O) 0.556(H ₂ O)	C ₆₀ H ₉₂ N ₁₂ O ₂₀
Formula weight	1250.52	1477.66	1431.72	1301.46
System	Monoclinic	Monoclinic	Triclinic	Monoclinic
Space group	<i>P</i> 2 ₁ /c	<i>P</i> 2 ₁ /n	<i>P</i> 1̄	<i>P</i> 2 ₁ /c
a (Å)	10.1468(17)	11.7433(3)	11.5603(5)	9.9939(4)
b (Å)	19.626(4)	24.2497(7)	13.0290(5)	23.5910(9)
c (Å)	18.398(5)	13.9071(4)	14.4868(6)	14.8973(6)
α (°)	90	90	105.275(1)	90
β (°)	98.846(17)	100.563(1)	108.615(2)	93.357(3)
γ (°)	90	90	99.629(2)	90
V(Å³)	3620.2(14)	3893.23(19)	1917.90(14)	3506.3(2)
Z	2	2	1	2
D_x (g cm⁻³)	1.047	1.260	1.240	1.233
λ (Å)	1.54178	1.54178	1.54178	1.54178
μ (mm⁻¹)	0.616	0.799	0.779	0.776
F₀₀₀	1200.0	1584.0	770.0	1392.0
R1 (I > 2σI)	0.0660(4433)	0.0557(4919)	0.0521(5414)	0.0923(2488)
wR₂	0.1969(6577)	0.1688(7289)	0.1561(7207)	0.2268(4907)
N. of param.	399	430	470	458
GooF	1.043	1.051	1.040	1.083
ρ_{min}, ρ_{max} (eÅ⁻³)	-0.23, 0.22	-0.26, 0.31	-0.25, 0.25	-0.17, 0.27
Restraints	/	/	3	/

Table S2. Torsion angles for compounds **1**, **2**, **3** and **4**.^a

Compound	ω_1 C11-C12-N1-C1	ω_2 C1-C2-N2-C3	ω_3 C3-C4-N3-C5	ω_4 C5-C6-N4-C7	ω_5 C7-C8-N5-C9	ω_6 C9-C10-N6-C11
1	-11.5(3)	-8.4(3)	-2.0(3)	12.4(3)	22.1(4)	-176.2(2)
2	-17.1(3)	-5.6(3)	-3.0(3)	15.6(3)	18.0(3)	177.1(2)
3	-20.5(2)	-1.5(3)	-0.8(3)	21.1(3)	17.4(3)	179.5(2)
4	-11.1(8)	-6.5(8)	-7.0(7)	18.9(8)	7(1)	179.2(5)

Compound	ϕ_1 C12-N1-C1-C2	ϕ_2 C2-N2-C3-C4	ϕ_3 C4-N3-C5-C6	ϕ_4 C6-N4-C7-C8	ϕ_5 C8-N5-C9-C10	ϕ_6 C10-N6-C11-C12
1	-73.8(3)	-78.2(3)	83.0(3)	84.8(3)	76.8(3)	-77.3(3)
2	-80.2(2)	-92.3(2)	106.4(2)	80.3(3)	74.6(2)	-70.1(2)
3	-71.7(2)	-93.3(2)	94.7(2)	80.5(2)	72.3(2)	-66.5(2)
4	-69.8(6)	-82.6(6)	96.8(6)	78.3(7)	85.0(8)	-60.3(6)

Compound	ψ_1 N1-C1-C2-N2	ψ_2 N2-C3-C4-N3	ψ_3 N3-C5-C6-N4	ψ_4 N4-C7-C8-N5	ψ_5 N5-C9-C10-N6	ψ_6 N6-C11-C12-N1
1	-171.6(2)	178.8(2)	-168.2(2)	-168.1(2)	174.8(2)	170.4(2)
2	-175.7(2)	-174.3(2)	-170.5(2)	-175.1(2)	169.4(2)	167.5(2)
3	178.8(2)	-179.8(2)	-169.7(2)	-175.7(2)	173.3(2)	159.5(2)
4	-169.3(5)	-175.8(5)	-158.9(5)	-170.8(6)	-169.1(5)	146.1(5)

Compound	χ_{1-1} C12-N1-C13-C14	χ_{1-2}^b C2-N2-C16-C17	χ_{1-3}^c C4-N3-C19-C20	χ_{1-4} C6-N4-C22-C23	χ_{1-5} C8-N5-C25-C26	χ_{1-6} C10-N6-C28-C29
1	-129.5(2)	-81(1)	-90.6(3)	93.6(3)	160.1(3)	-92.2(3)
2	-115.8(3)	-88.8(3)	137.1(2)	107.8(2)	-91.5(3)	-98.0(2)
3	-145.3(2)	-86.2(4)	118.1(4)	98.1(2)	-87.9(3)	-96.9(2)
4	100.3(7)	-114.3(7)	125.8(6)	109.5(8)	140.8(8)	93.8(7)

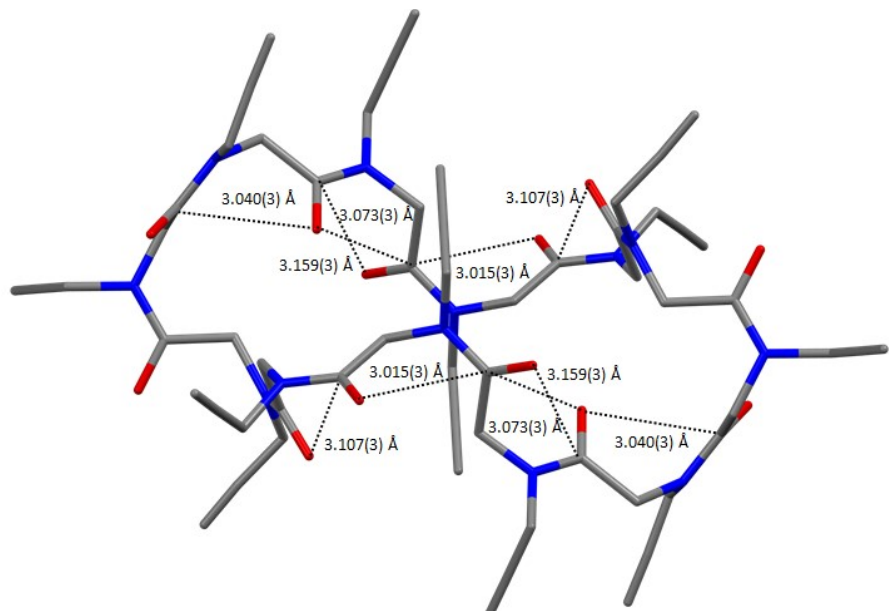
^a The other six residues have identical values with opposite signs because of the crystallographic inversion centre.

^b χ_{1-2} is the χ_1 angle for the second residue, for compounds **1** and **3** it refers to the atoms with the highest occupancy factor, namely C2-N2-C16-C17A atoms.

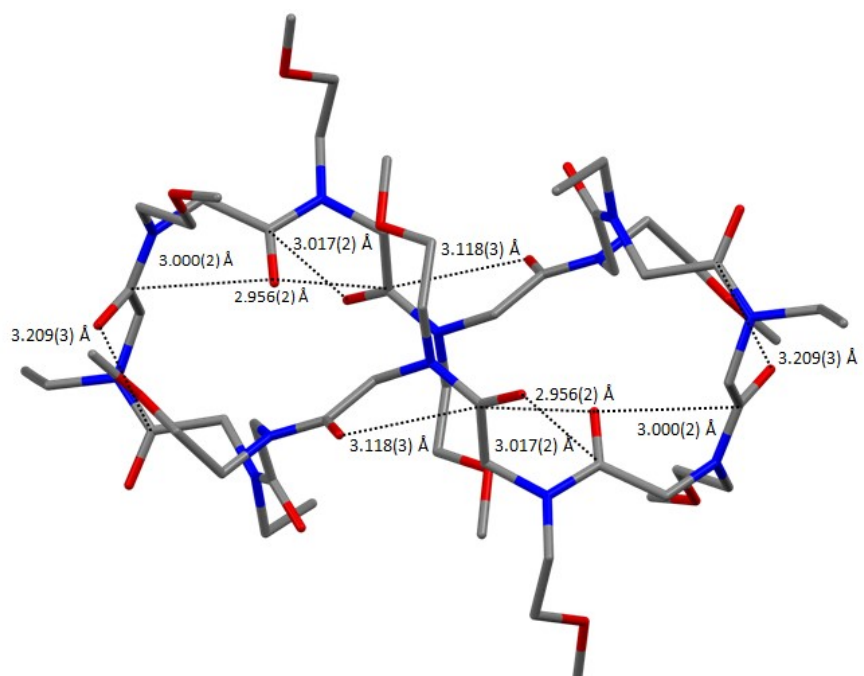
^c χ_{1-3} is the χ_1 angle for the third residue, for compound **3** it refers to the atoms with the highest occupancy factor, namely C4-N3-C19A-C20A atoms.

5.2 Intramolecular interactions

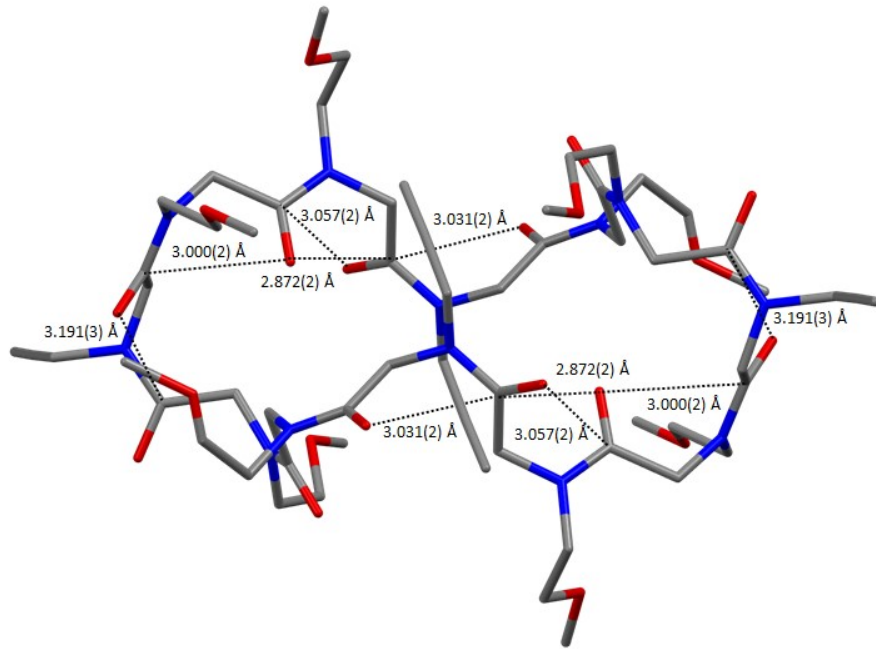
5.2.1 CO···CO interactions



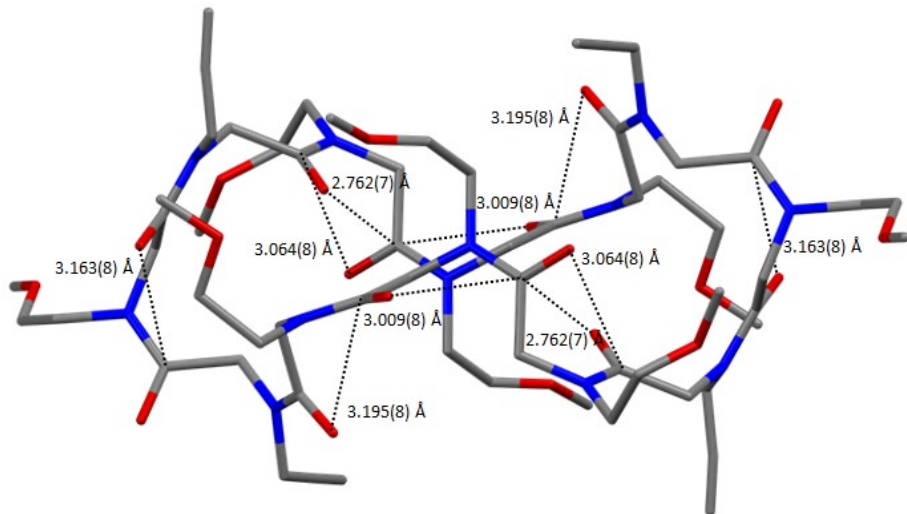
(a)



(b)



(c)



(d)

Figure S2. Backbone conformation of **1** (a), **2** (b), **3** (c) and **4** (d) and one-sided and reciprocal CO...CO interactions in the macrocycles, as shown by CO...CO distances below 3.22 Å. Hydrogen atoms omitted for clarity. For clarity, only the atoms with the highest occupancy factor are shown.

Table S3. CO···CO distances and corresponding θ angles for compounds **1**, **2**, **3** and **4**.

Compound	d1_2 (Å)	d2_1 (Å)	d2_3 (Å)	d3_2 (Å)	d3_4 (Å)	d4_3 (Å)
1	4.205(3)	3.107(3)	4.337(4)	3.336(3)	4.221(3)	3.266(3)
2	4.359(3)	3.327(3)	4.484(3)	3.640(3)	4.213(3)	3.209(3)
3	4.379(3)	3.368(3)	4.395(3)	3.512(3)	4.172(3)	3.191(3)
4	4.309(6)	3.195(8)	4.453(7)	3.599(6)	4.177(8)	3.163(8)

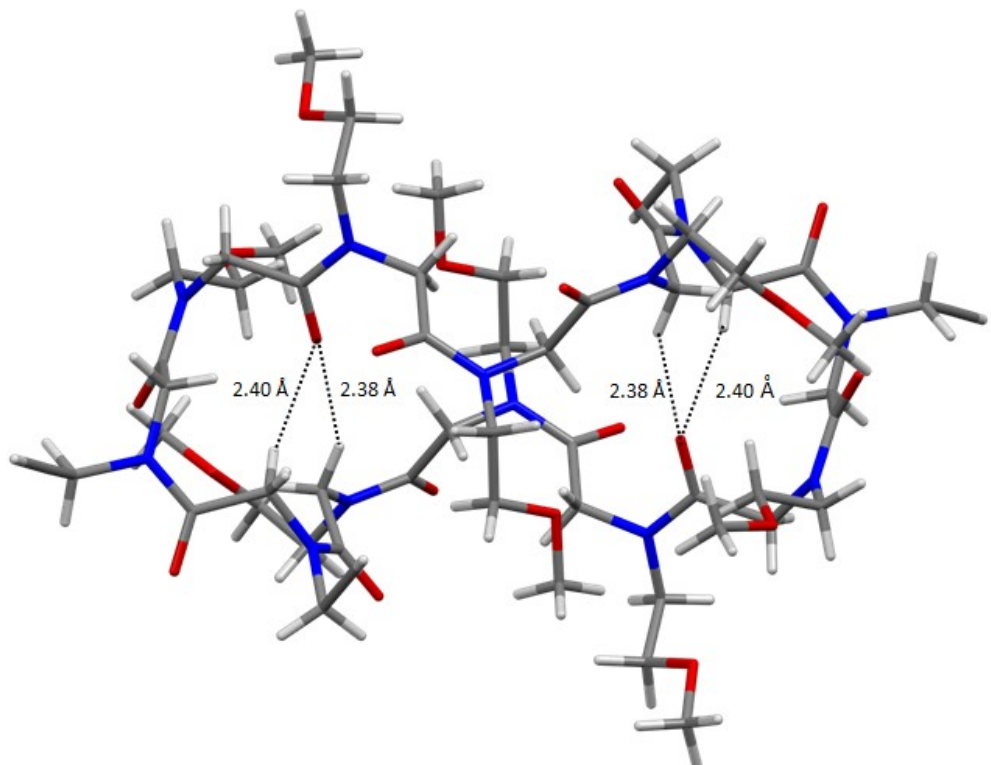
Compound	d4_5 (Å)	d5_4 (Å)	d5_6 (Å)	d6_5 (Å)	d6_1 (Å)	d1_6 (Å)
1	4.089(3)	3.040(3)	3.073(3)	3.159(3)	4.187(3)	3.015(3)
2	4.145(2)	3.000(2)	2.956(2)	3.017(2)	4.183(3)	3.118(3)
3	4.138(2)	3.000(2)	2.872(2)	3.057(2)	4.114(2)	3.031(2)
4	4.264(8)	3.297(8)	2.762(7)	3.064(8)	4.214(8)	3.009(8)

Compound	θ_{4_5} (°)	θ_{5_4} (°)	θ_{5_6} (°)	θ_{6_5} (°)	θ_{6_1} (°)	θ_{1_6} (°)
1	67.0(2)	122.2(2)	76.8(1)	130.9(2)	71.2(2)	118.5(2)
2	71.5(1)	124.1(2)	81.3(2)	125.6(2)	68.8(1)	118.7(2)
3	73.6(1)	125.4(1)	80.0(1)	126.4(1)	67.3(1)	115.2(2)
4	68.5(3)	124.5(4)	83.6(3)	130.0(4)	67.1(4)	116.9(4)

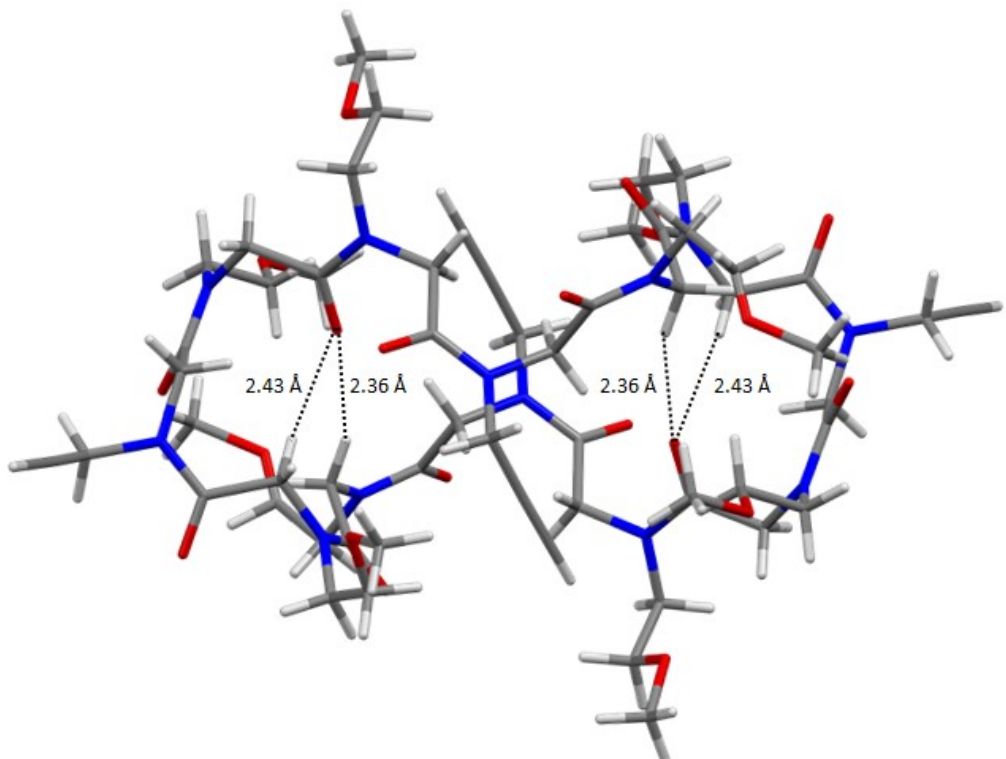
Compound	θ_{4_5} (°)	θ_{5_4} (°)	θ_{5_6} (°)	θ_{6_5} (°)	θ_{6_1} (°)	θ_{1_6} (°)
1	62.9(2)	113.1(2)	86.2(2)	82.3(1)	64.0(1)	122.0(2)
2	62.8(1)	118.9(1)	84.2(1)	81.5(1)	65.1(1)	116.9(1)
3	63.4(1)	119.5(1)	87.5(1)	79.0(1)	63.0(1)	115.4(1)
4	72.1(3)	120.1(5)	93.3(4)	79.3(3)	64.8(3)	126.0(4)

CO···CO distances and relative θ angles of the molecular structures of compounds **1**, **2**, **3** and **4**. In particular, d1_2 = O1...C4, d2_1 = O2...C2, d2_3 = O2...C6, d3_2 = O3...C4, d3_4 = O3...C8, d4_3 = O4...C6, d4_5 = O4...C10, d5_4 = O5...C8, d5_6 = O5...C12, d6_5 = O6...C10, d6_1 = O6...C2, d1_6 = O1...C12, θ_{1_2} = O1...C4-O2, θ_{2_1} = O2...C2-O1, θ_{2_3} = O2...C6-O3, θ_{3_2} = O3...C4-O2, θ_{3_4} = O3...C8-O4, θ_{4_3} = O4...C6-O3, θ_{4_5} = O4...C10-O5, θ_{5_4} = O5...C8-O4, θ_{5_6} = O5...C12-O6, θ_{6_5} = O6...C10-O5, θ_{6_1} = O6...C2-O1, θ_{1_6} = O1...C12-O6.

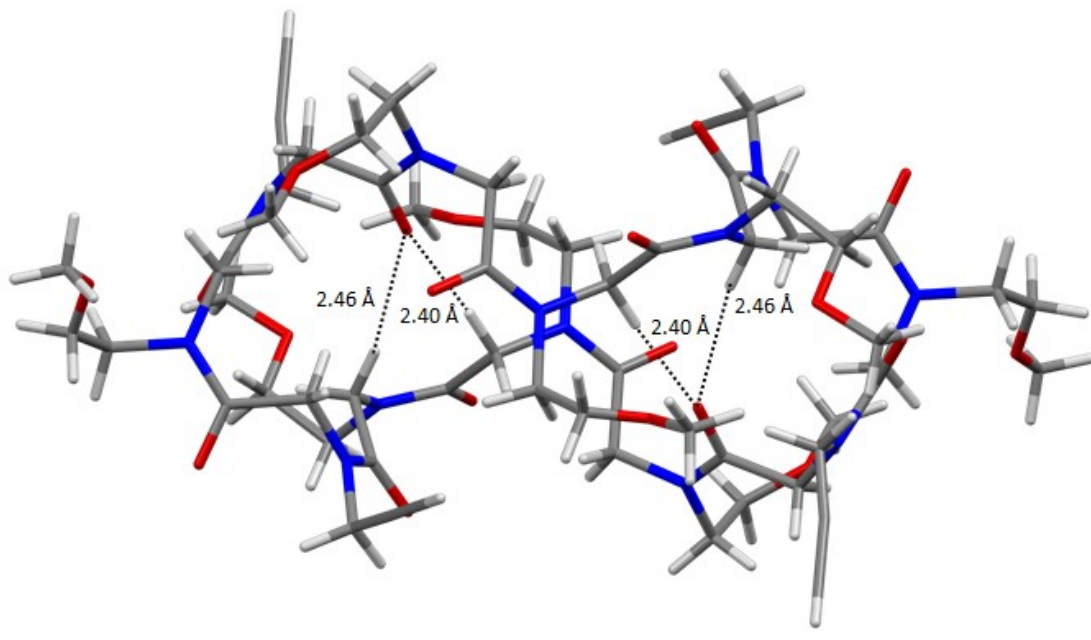
5.2.2 Backbone CH···OC hydrogen bonds



(a)



(b)



(c)

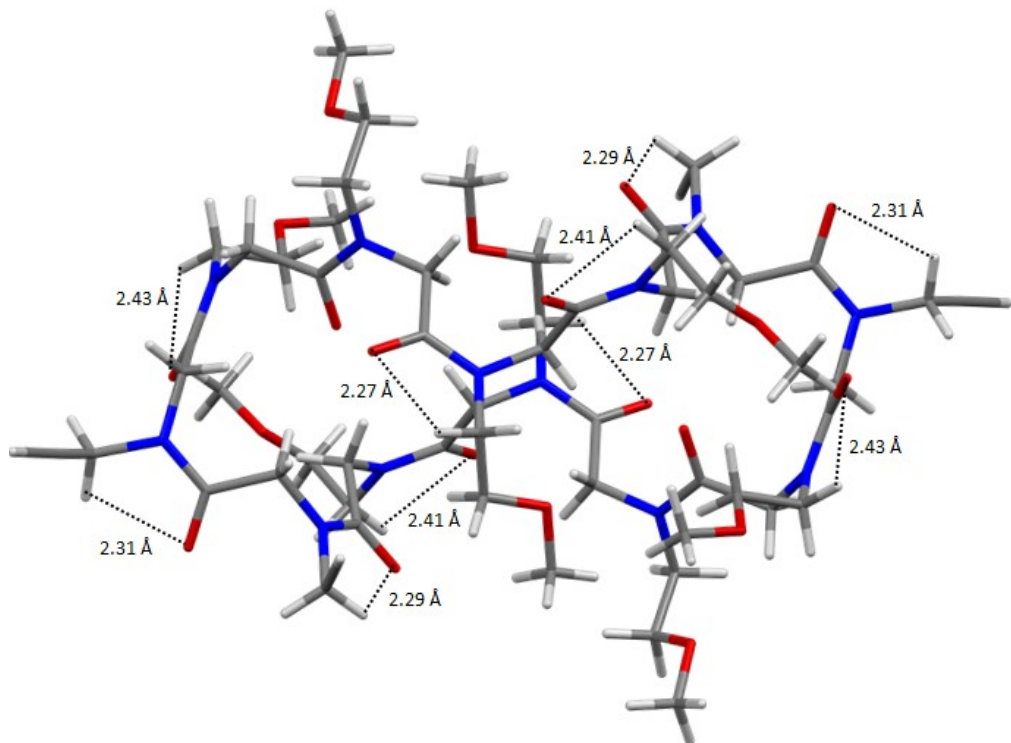
Figure S3. Backbone CH···OC hydrogen bonds between *trans* residues carbonyl groups and opposite methylene hydrogen atoms in crystal structures of **2** (a), **3** (b) and **4** (c). For clarity, only the atoms with the highest occupancy factor are shown.

Table S4. List of backbone intramolecular CH···OC hydrogen bond distances (\AA) and angles ($^{\circ}$).^a

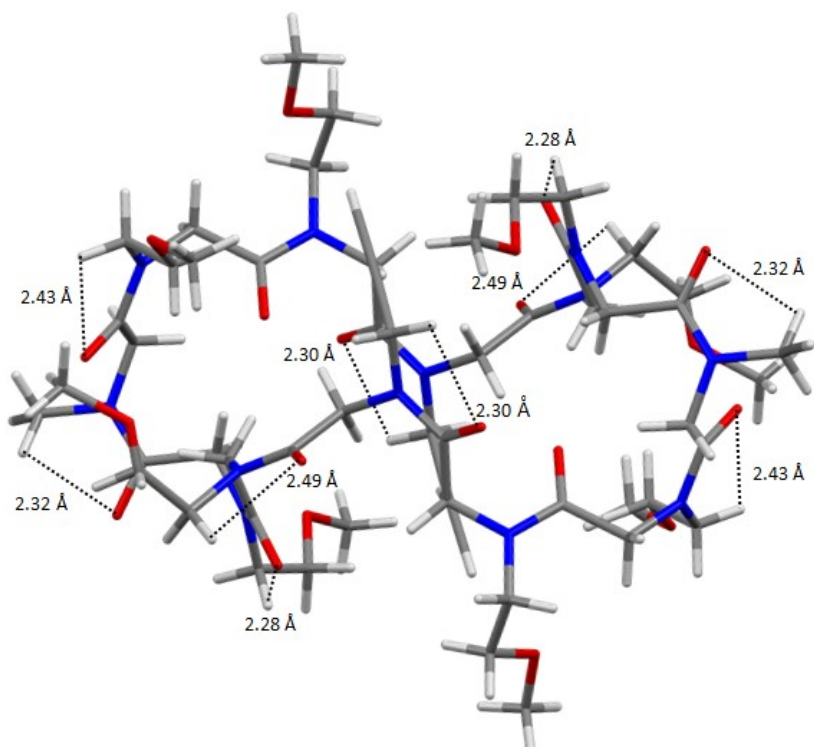
Crystal structure	D–H···A	D···A (\AA)	H···A (\AA)	D–H···A ($^{\circ}$)
1	C3–H3B···O5	3.298(3)	2.34	168.3
	C5–H5A···O5	3.311(3)	2.37	164.2
2	C3–H3B···O5	3.237(3)	2.38	147.7
	C5–H5A···O5	3.300(3)	2.40	153.9
3	C3–H3B···O5	3.273(2)	2.36	157.3
	C5–H5A···O5	3.369(3)	2.43	163.4
4	C1–H1A···O5	3.350(6)	2.40	168.1
	C3–H3B···O5	3.414(6)	2.46	168.6

^a As a consequence of the crystallographic inversion centre the same interactions occur twice.

5.2.3 Intramolecular C5 CH...OC interactions



(a)



(b)

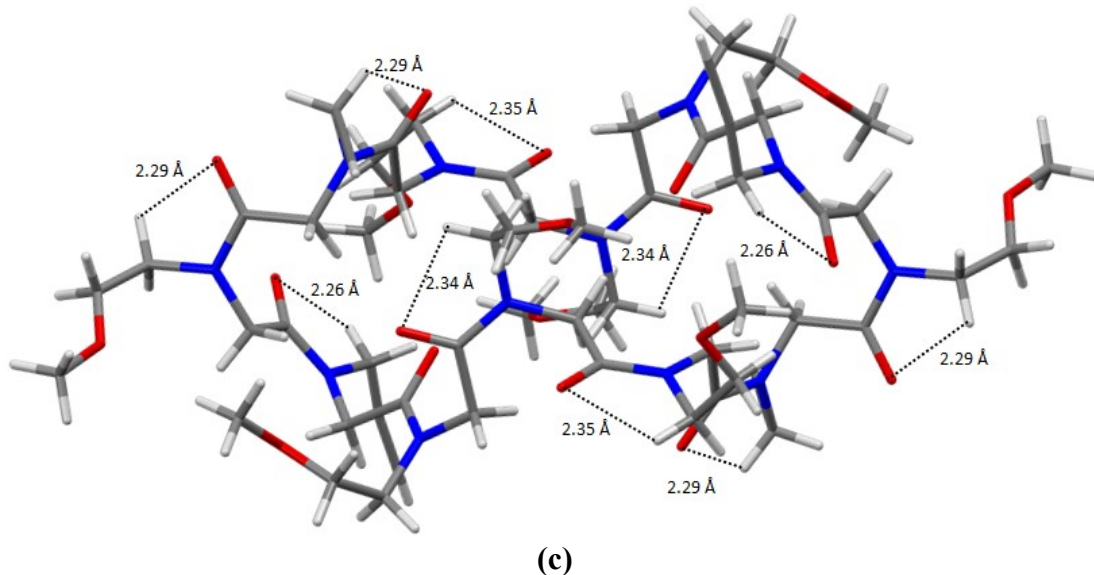


Figure S4. C5 CH···OC hydrogen bonds in crystal structures of **2** (a), **3** (b) and **4** (c). For clarity, only the atoms with the highest occupancy factor are shown.

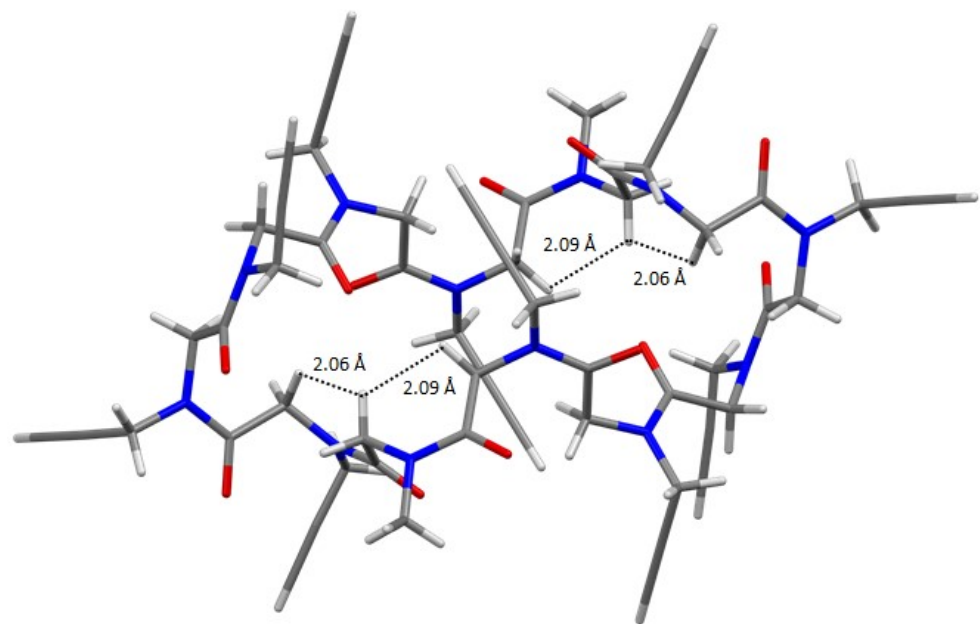
Table S5. List of intramolecular C5 CH···OC hydrogen bond distances (\AA) and angles ($^{\circ}$).^{a,b}

Compound	D–H···A	D···A (\AA)	H···A (\AA)	D–H···A ($^{\circ}$)	Side chain type
1	C16–H16A···O1	2.679(4)	2.47	91.6	Propargyl
	C19–H19A···O2	2.728(4)	2.41	98.8	Propargyl
	C22–H22B···O3	2.702(4)	2.36	100.0	Propargyl
	C25–H25B···O4	2.655(3)	2.34	98.0	Propargyl
	C13–H13A···O6	2.717(4)	2.28	106.5	Propargyl
2	C16–H16B···O1	2.718(3)	2.41	97.8	Methoxyethyl
	C19–H19B···O2	2.709(4)	2.29	105.3	Propargyl
	C22–H22A···O3	2.721(3)	2.31	104.6	Propargyl
	C25–H25B···O4	2.743(3)	2.43	98.6	Methoxyethyl
	C13–H13B···O6	2.716(3)	2.27	107.1	Methoxyethyl
3	C16–H16B···O1	2.751(2)	2.49	95.3	Methoxyethyl
	C19A–H19B···O2	2.736(4)	2.28	108.0	Methoxyethyl
	C22–H22B···O3	2.696(3)	2.32	102.0	Propargyl
	C25–H25B···O4	2.727(3)	2.43	97.4	Methoxyethyl
	C13–H13A···O6	2.702(3)	2.30	103.6	Propargyl
4	C16–H16B···O1	2.765(8)	2.35	105.2	Methoxyethyl
	C19–H19B···O2	2.735(8)	2.29	107.1	Propargyl
	C22–H22B···O3	2.711(8)	2.29	105.4	Methoxyethyl
	C25–H25B···O4	2.69(1)	2.26	105.9	Propargyl
	C13–H13A···O6	2.729(6)	2.34	103.4	Methoxyethyl

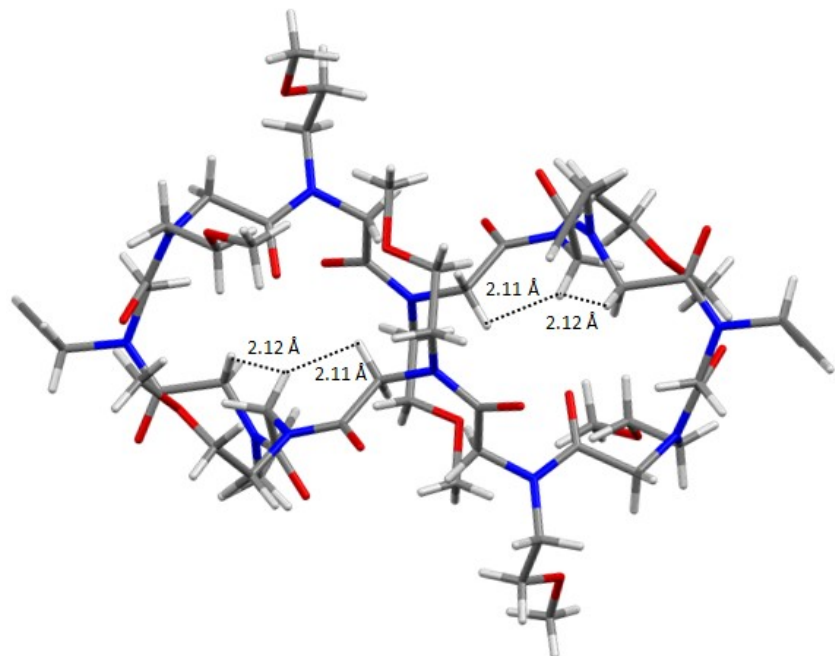
^a As a consequence of the crystallographic inversion centre the same interactions occur twice.

^b For the side chains showing positional disorder, we report only the CO···HC hydrogen bond distances and angles for the atoms with the highest occupancy factors.

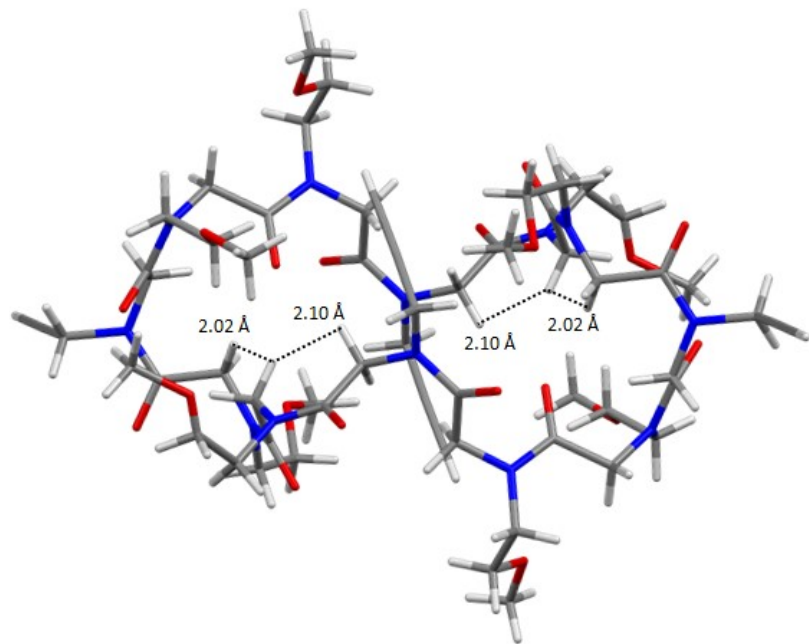
5.2.4 Intramolecular C6 CH...HC contacts



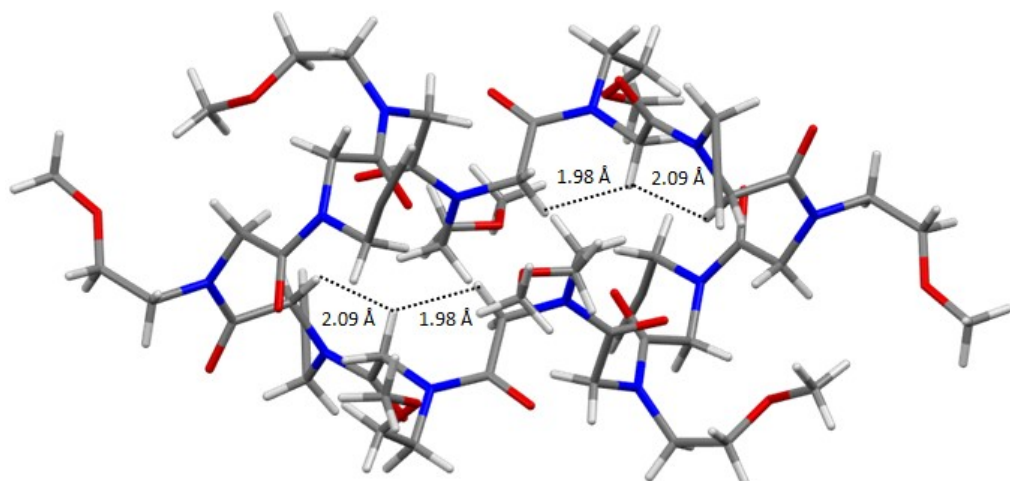
(a)



(b)



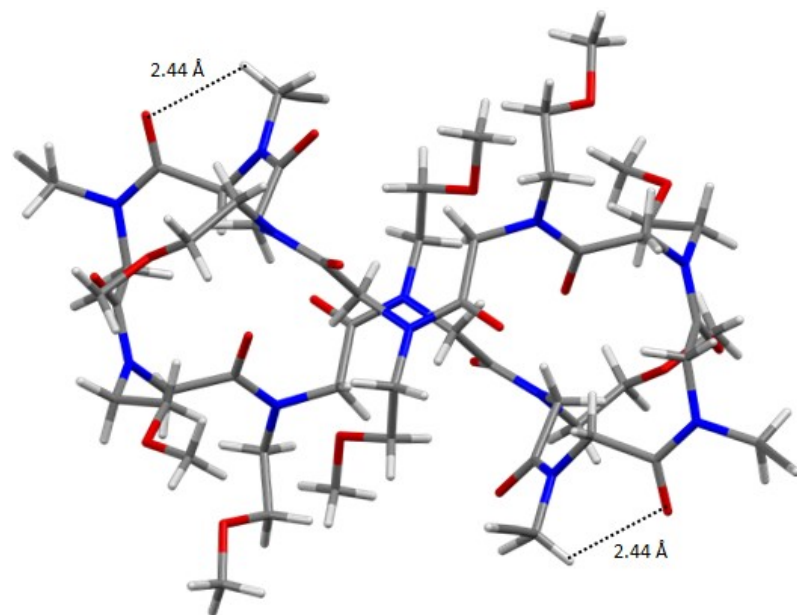
(c)



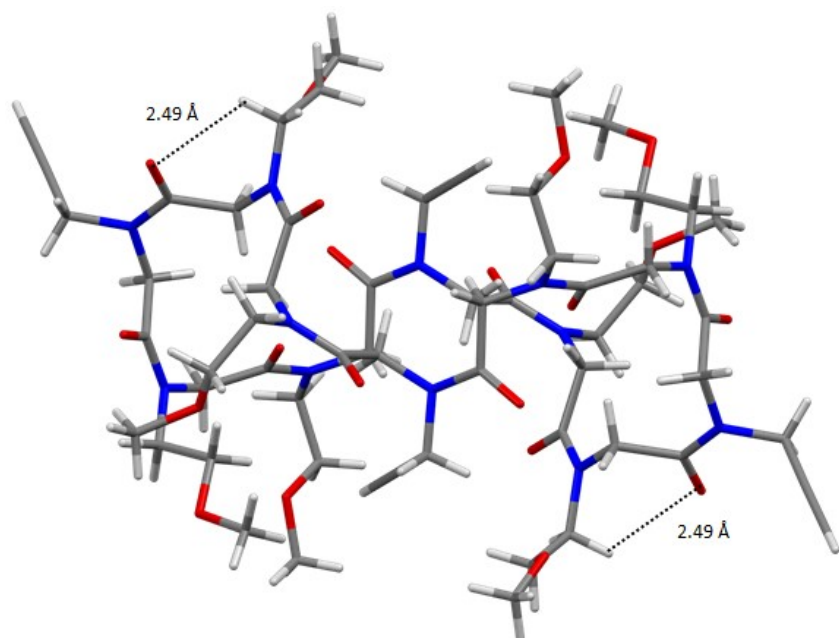
(d)

Figure S5. C6 CH...HC contacts in **1** (a), **2** (b), **3** (c) and **4** (d). For clarity, only the atoms with the highest occupancy factor are shown.

5.2.5 Intramolecular C6 CH \cdots OC interactions



(a)



(b)

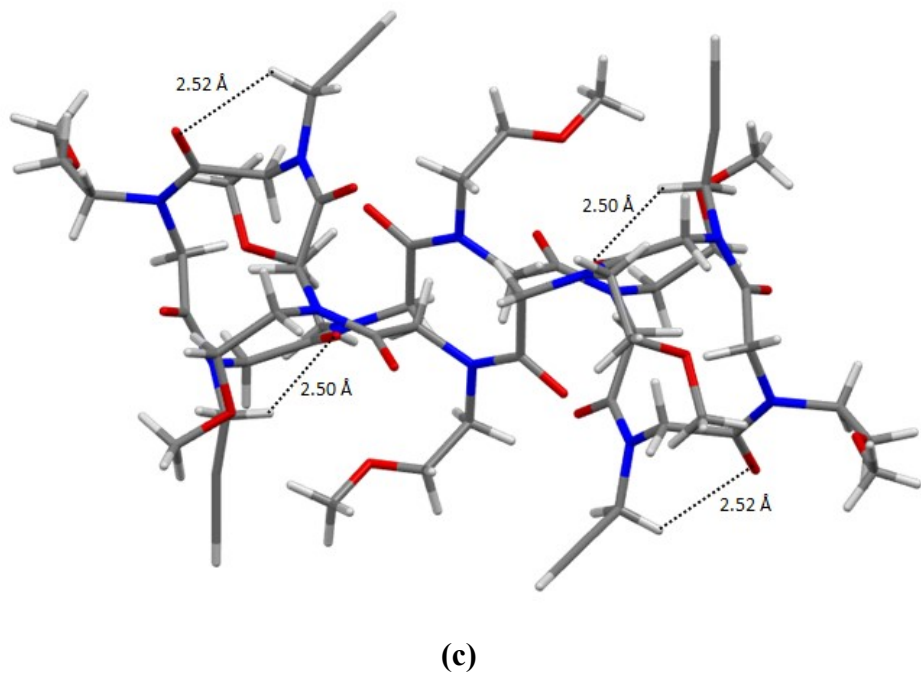


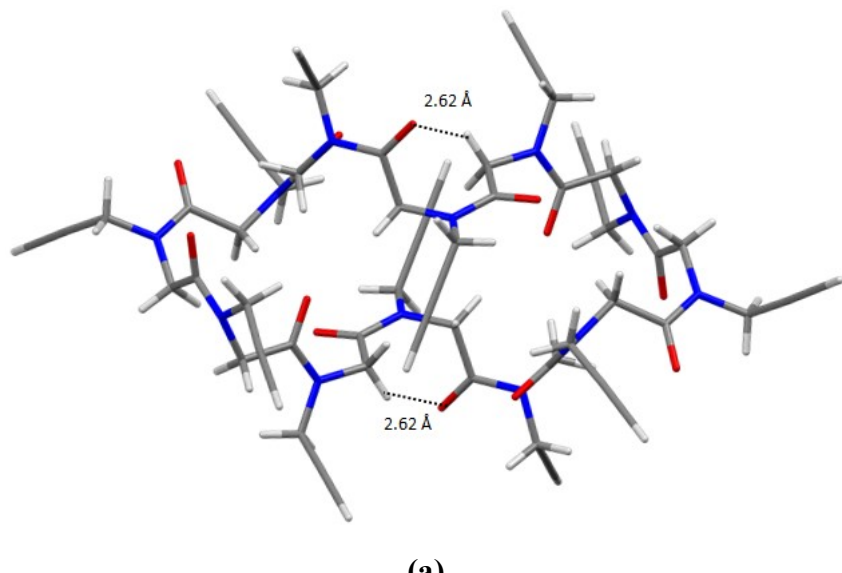
Figure S6. C6 CH \cdots OC hydrogen bonds in **2** (a), **3** (b) and **4** (c). For clarity, only the atoms with the highest occupancy factor are shown.

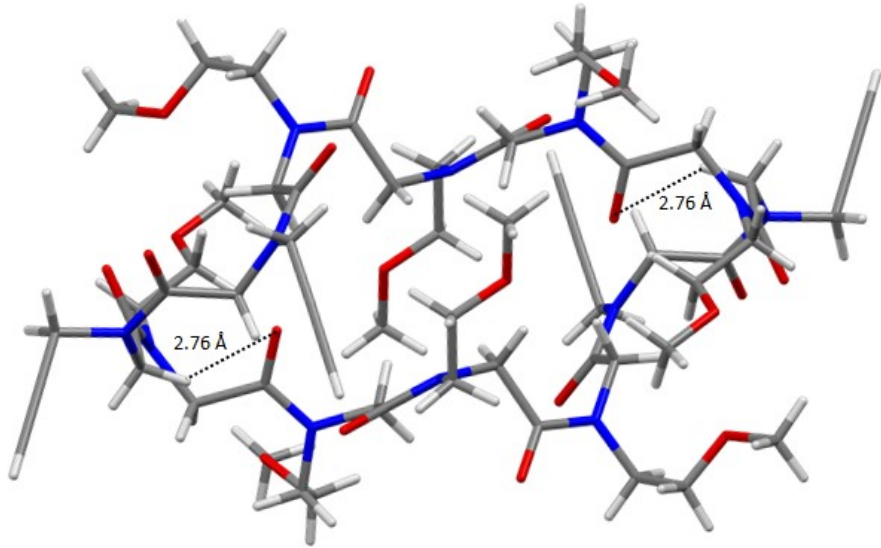
Table S6. List of backbone intramolecular CH \cdots OC hydrogen bond distances (\AA) and angles ($^{\circ}$) ^a

Crystal structure	D–H \cdots A	D \cdots A (\AA)	H \cdots A (\AA)	D–H \cdots A ($^{\circ}$)
2	C19–H19A \cdots O3	2.973(4)	2.44	114.5
3	C19–H19A \cdots O3	3.090(3)	2.49	120.1
4	C19–H19A \cdots O3	3.076(8)	2.52	116.6
	C25–H25A \cdots O5	3.044(9)	2.50	115.6

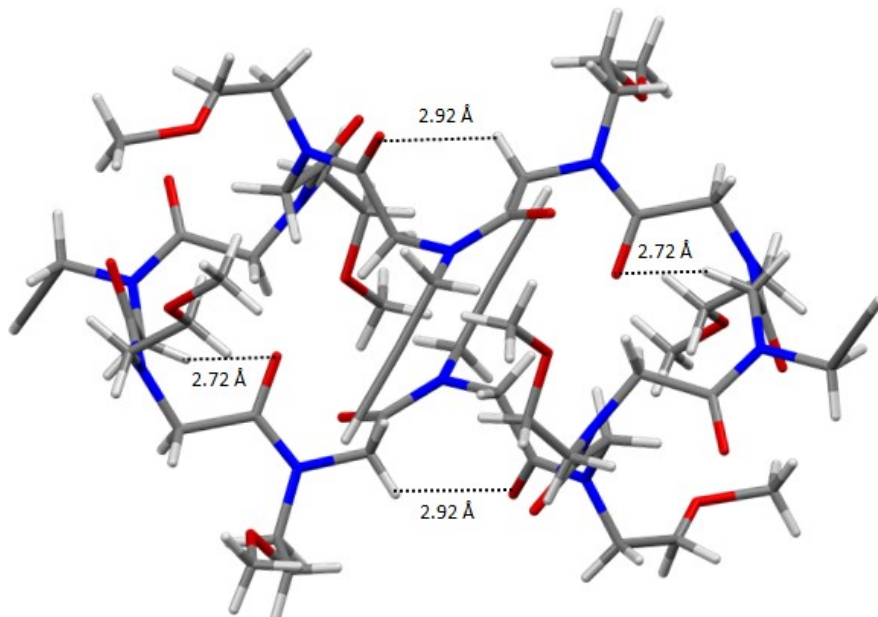
^a As a consequence of the crystallographic inversion centre the same interactions occur twice.

5.2.6 Intramolecular C7 CH \cdots OC interactions





(b)



(c)

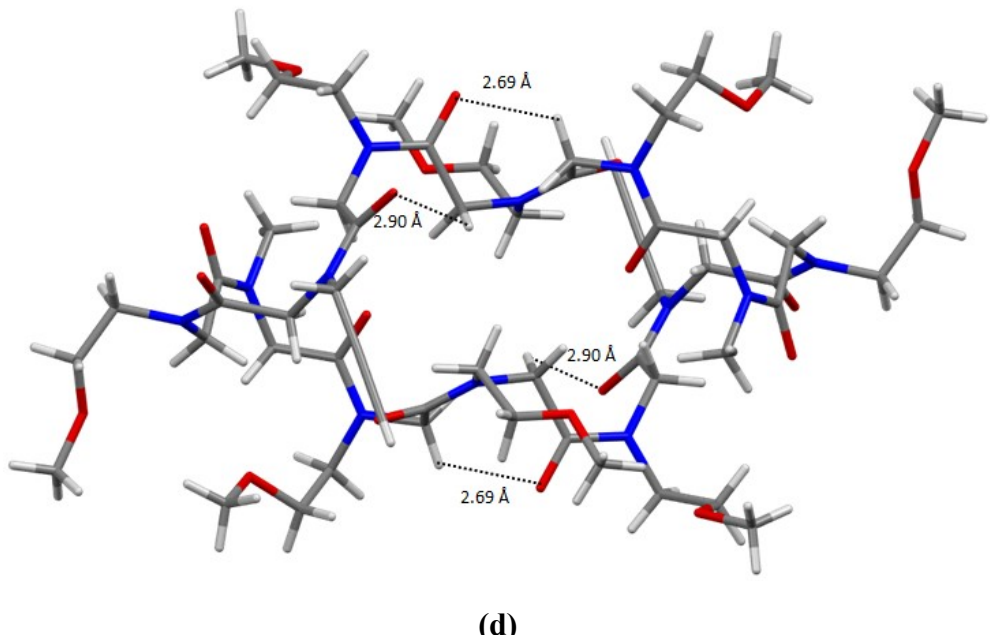


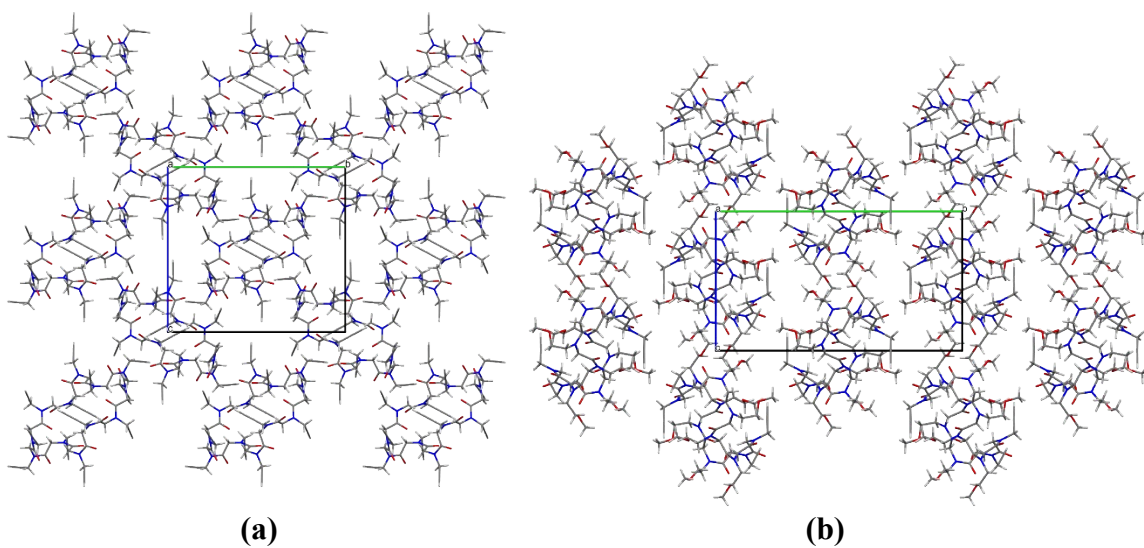
Figure S7. C7 CH···OC hydrogen bonds in **1** (a), **2** (b), **3** (c) and **4** (d). For clarity, only the atoms with the highest occupancy factor are shown.

Table S7. List of backbone intramolecular CH \cdots OC hydrogen bond distances (\AA) and angles ($^\circ$) ^a

Crystal structure	D–H···A	D···A (Å)	H···A (Å)	D–H···A (°)
1	C11–H11A···O1	3.240(4)	2.62	122.2
2	C7–H7A···O5	3.344(3)	2.76	119.5
3	C11–H11A···O1	3.435(2)	2.92	114.0
	C7–H7A···O5	3.313(2)	2.72	120.4
4	C11–H11A···O1	3.152(7)	2.69	109.9
	C1–H1B···O2	3.487(6)	2.90	119.9

^a As a consequence of the crystallographic inversion centre the same interactions occur twice.

5.3 Crystal packing



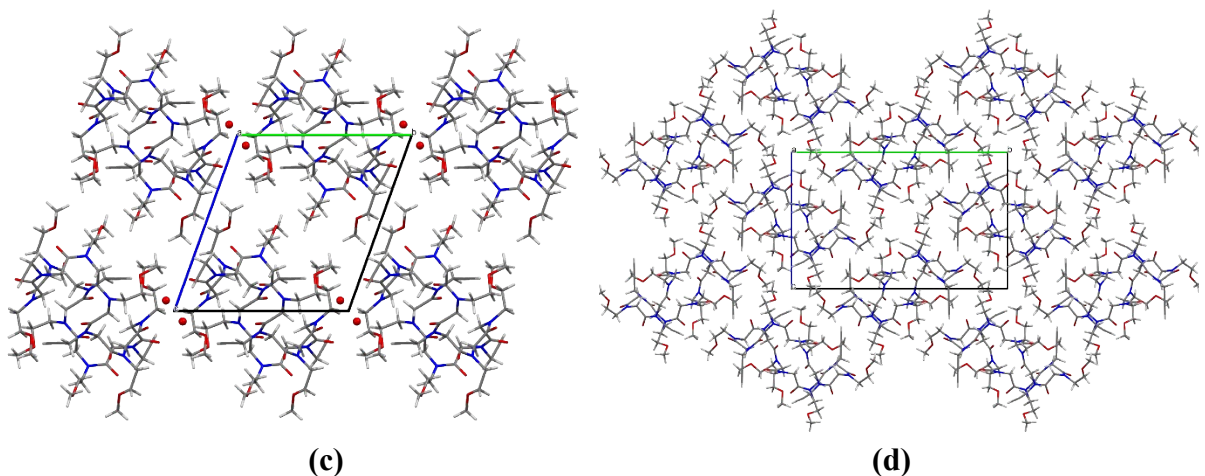


Figure S8. Crystal packing of compounds **1** (a), **2** (b), **3** (c), and **4** (d) along the *a* axis. For clarity, only the atoms with the highest occupancy factor are shown. Water molecules in **3** are depicted in ball and stick style.

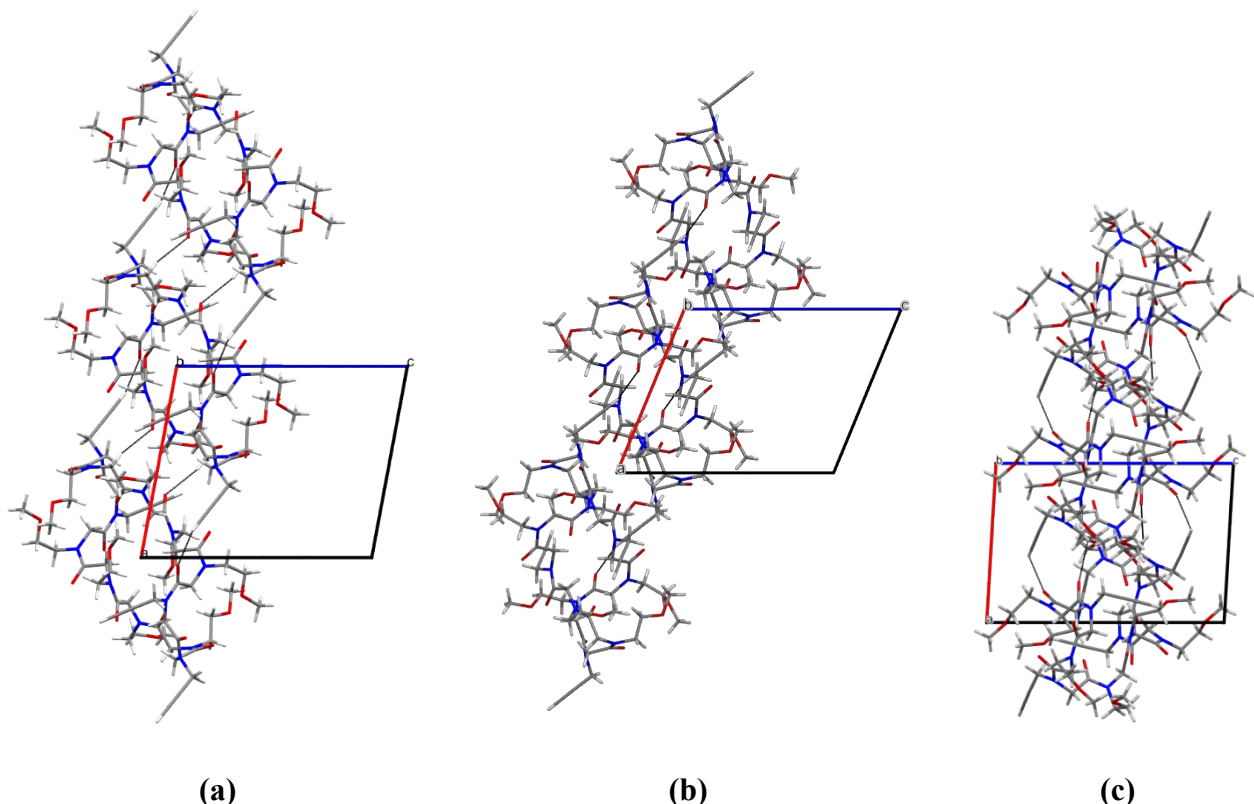


Figure S9. Cyclic peptoids columns in the crystal structures of **2**, **3** and **4** (view along the *b* axis). Solvent molecules are omitted for clarity and only the atoms with the highest occupancy factor are shown. For clarity, only the atoms with the highest occupancy factor are shown.

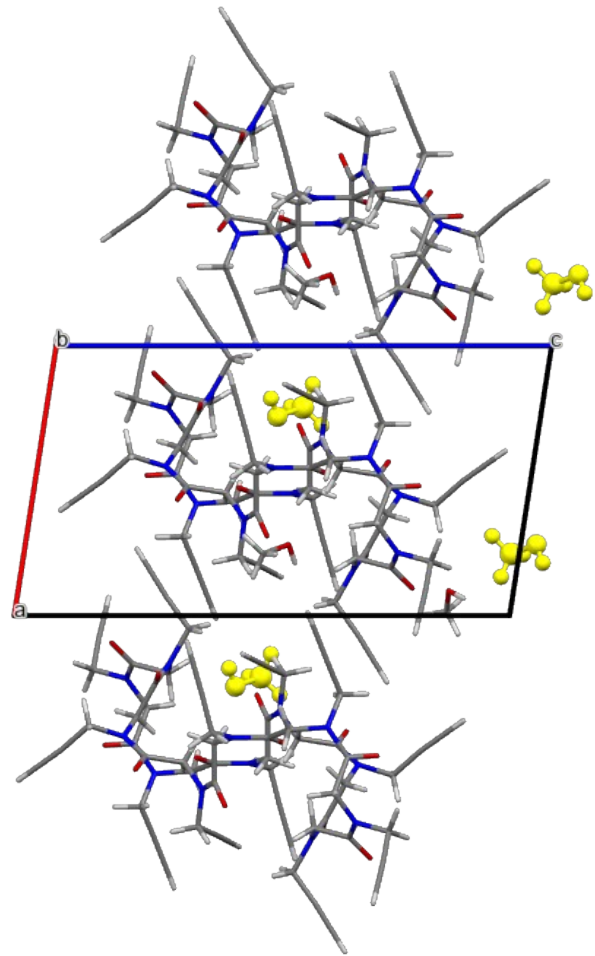
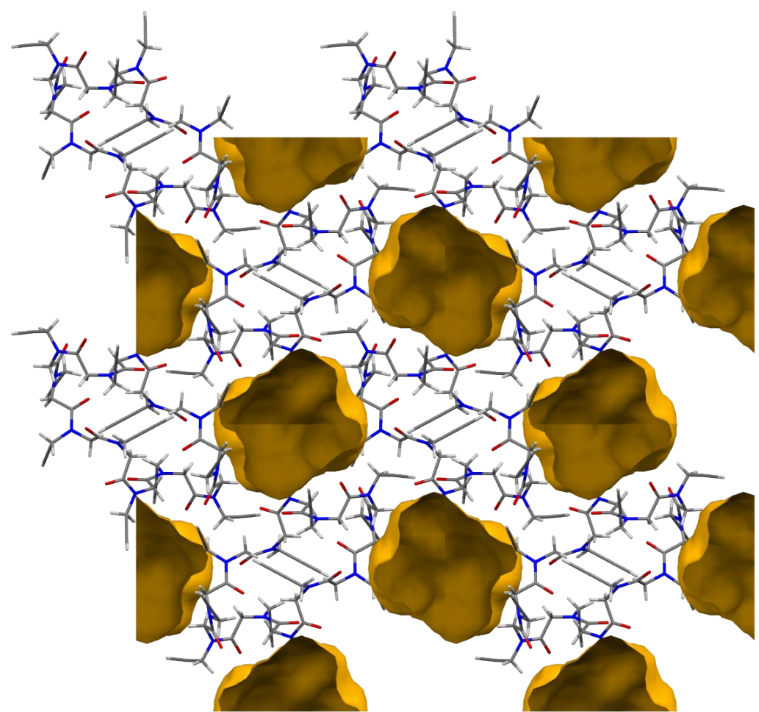
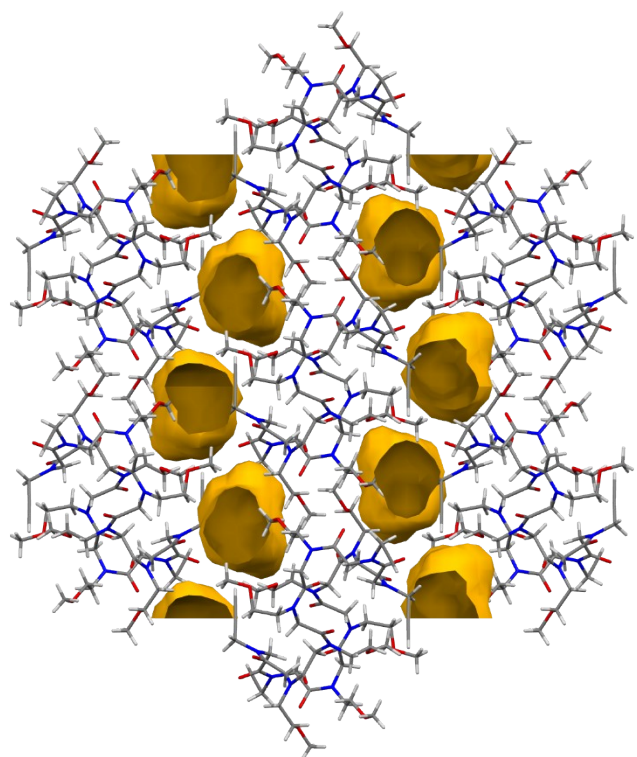


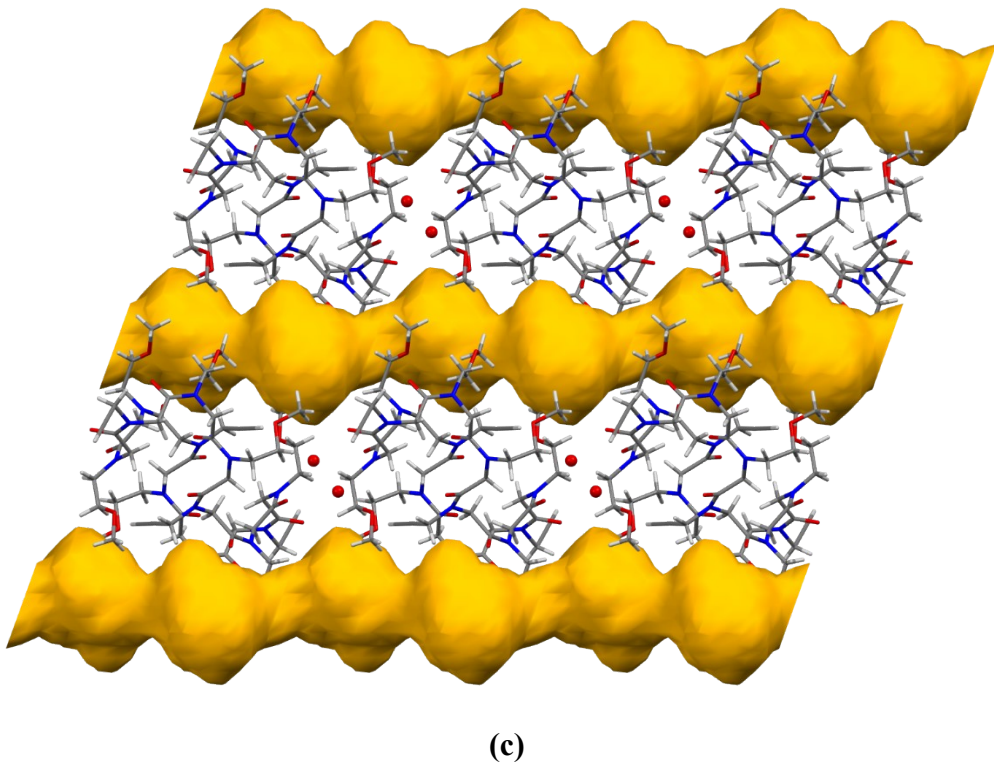
Figure S10. Cyclic peptoids columns in the crystal structure of **1** (view along the *b* axis). The methanol molecules bridging together the host molecules are depicted in yellow. Disordered guest molecules have been omitted for clarity and the disordered side chains are shown only the atoms with the highest occupancy factor. For clarity, only the atoms with the highest occupancy factor are shown.



(a)



(b)



(c)

Figure S11. Crystal packing of **1** (a), **2** (b) and **3** (c) with cavities and channels represented in yellow. Voids were calculated using the default options in Mercury⁵ (probe radius: 1.2 Å and grid spacing: 0.7 Å) giving the following results: 660.86 Å³ in crystal structure of compound **1** (18.3% of unit cell volume), 526.08 Å³ in crystal structure of compound **2** (13.5% of unit cell volume) and 231.57 Å³ in crystal structure of compound **3** (12.1% of unit cell volume). For clarity, only the atoms with the highest occupancy factor are shown.

6.0 Quantum Mechanical Computations

The nature of non-covalent interactions in cyclo-(Npa)₁₂ **1** was investigated by QTAIM,⁶ searching for bond critical points (BCPs), using the SYSMOIC package,⁷ taking as inputs the wavefunction files obtained by Gaussian16.⁸ Computations have been performed either taking the X-ray geometry, or fully optimizing the geometry at the same level used for the QTAIM analysis; the following computations were performed:

- 1) B3LYP/6-311G(d,p)//B3LYP/6-311G(d,p)
- 2) B3LYP/6-311G(d,p)//X-ray
- 3) B3LYP/6-311+G(d,p)//B3LYP/6-311+G(d,p)

6.1 Interactions energies: Espinosa-Molins-Lecomte equation

Intramolecular interaction energies were calculated by means of the Espinosa-Molins-Lecomte (EML) equation.⁹ The equation calculates the dissociation energy as the negative of half the potential energy density at the BCP multiplied by a volume of 1 atomic unit. It was originally introduced for hydrogen bonded complexes but was also justified for other non-covalent complexes too.¹⁰ However,

it must be considered that the EML equation leads likely to too strong interactions in case of intramolecular hydrogen bonds.¹¹ Interaction energies stronger than 1 kcal mol⁻¹ have been plotted as a function of the density at the BCP in Figure S12. The BCPs corresponding to the C5 CH...CO interactions and their corresponding energies are present only for the B3LYP/6-311G(d,p)//B3LYP/6-311G(d,p) calculation (Table S8).

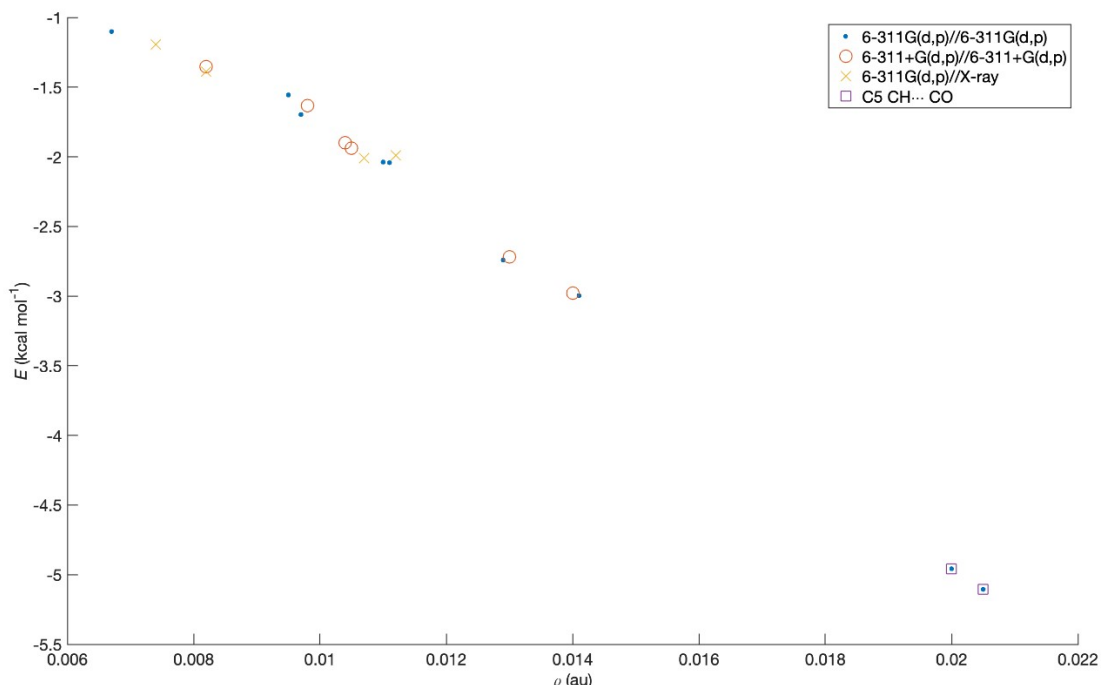


Figure S12. Interaction energy estimated with the EML equation for the BCP obtained with three different computations, all using the B3LYP functional. The densities at the BCP for the C5 CH...CO interactions, revealed as BCPs only at the B3LYP/6-311G(d,p)//B3LYP/6-311G(d,p) level, are highlighted by a square.

B3LYP/6-311G(d,p)//B3LYP/6-311G(d,p)					B3LYP/6-311+G(d,p)//B3LYP/6-311+G(d,p)					B3LYP/6	
X	Y	Z	RHO (au)	E (kcal/mol)	X	Y	Z	RHO (au)	E (kcal/mol)	X	Y
12.3744	1.7003	4.5018	0.0205	-5.1053							
for the interactions											
the text for 3 levels of											
Estimated interaction											
according to the Espinosa-											
equation are also given											
14.9865	4.9631	1.5498	0.0200	-4.9578							
7.3455	2.6279	0.4944	0.0141	-4.9578							
-7.3455	2.6279	0.4944	0.0141	-2.9965	7.3606	2.7667	0.4835	0.0140	-2.9801		
4.0859	2.1852	2.8099	0.0129	-2.7407	-7.3606	2.7667	0.4835	0.0140	-2.9801		
-4.0859	2.1852	2.8099	0.0129	-2.7407	4.0519	2.2447	2.8013	0.0130	-2.7180		
9.9926	7.0359	3.0601	0.0111	-2.0417	9.9302	7.0500	3.0618	0.0104	-1.8983		
-9.9926	7.0359	3.0601	0.0111	-2.0417	-9.9302	7.0500	3.0618	0.0104	-1.8983		
14.8940	1.4065	1.4246	0.0110	-2.0381	14.9229	1.5288	1.4666	0.0105	-1.9370		
-14.8940	1.4065	1.4246	0.0110	-2.0381	-14.9229	1.5288	1.4666	0.0105	-1.9370		
6.3115	0.4893	1.6936	0.0097	-1.6966	6.3244	0.5419	1.6070	0.0082	-1.3539	7.3839	0.8786
-6.3115	0.4893	1.6936	0.0097	-1.6966	-6.3244	0.5419	1.6070	0.0082	-1.3539	7.3838	0.8786
7.6622	0.1391	0.0580	0.0095	-1.5560	7.7530	0.1722	0.1028	0.0098	-1.6309	6.3614	0.3348
-7.6622	0.1391	0.0580	0.0095	-1.5560	-7.7530	0.1722	0.1028	0.0098	-1.6309	6.3614	0.3348
0.6521	5.1936	4.0012	0.0067	-1.1008						0.1381	4.8512
-0.6521	5.1936	4.0012	0.0067	-1.1008						0.1382	4.8513
										4.1552	1.1277
										4.1551	1.1277

Table S8. Location of BCP densities (in atomic units) for the interactions discussed in the text for 3 levels of computation. Estimated interaction energies according to the Espinosa-Molins-Lecomte equation are also given

6.2 Non-Covalent Interactions Analysis

The computation of s and the eigenvalues of the Hessian of the density in cubes of 2 bohr side centered on the BCPs with a step of 0.1 bohr gave the values used in the plots of Figure S13. When the BCP was missing (inset a, e and f) the cube was centered on the midpoint between the two interacting atoms. For all interactions considered the plots indicate an attractive interaction (leftmost peaks) and a repulsive interaction (rightmost peaks), which are associated with a BCP and an RCP in subplots b, c and d, but not ion subplots a, e and f.

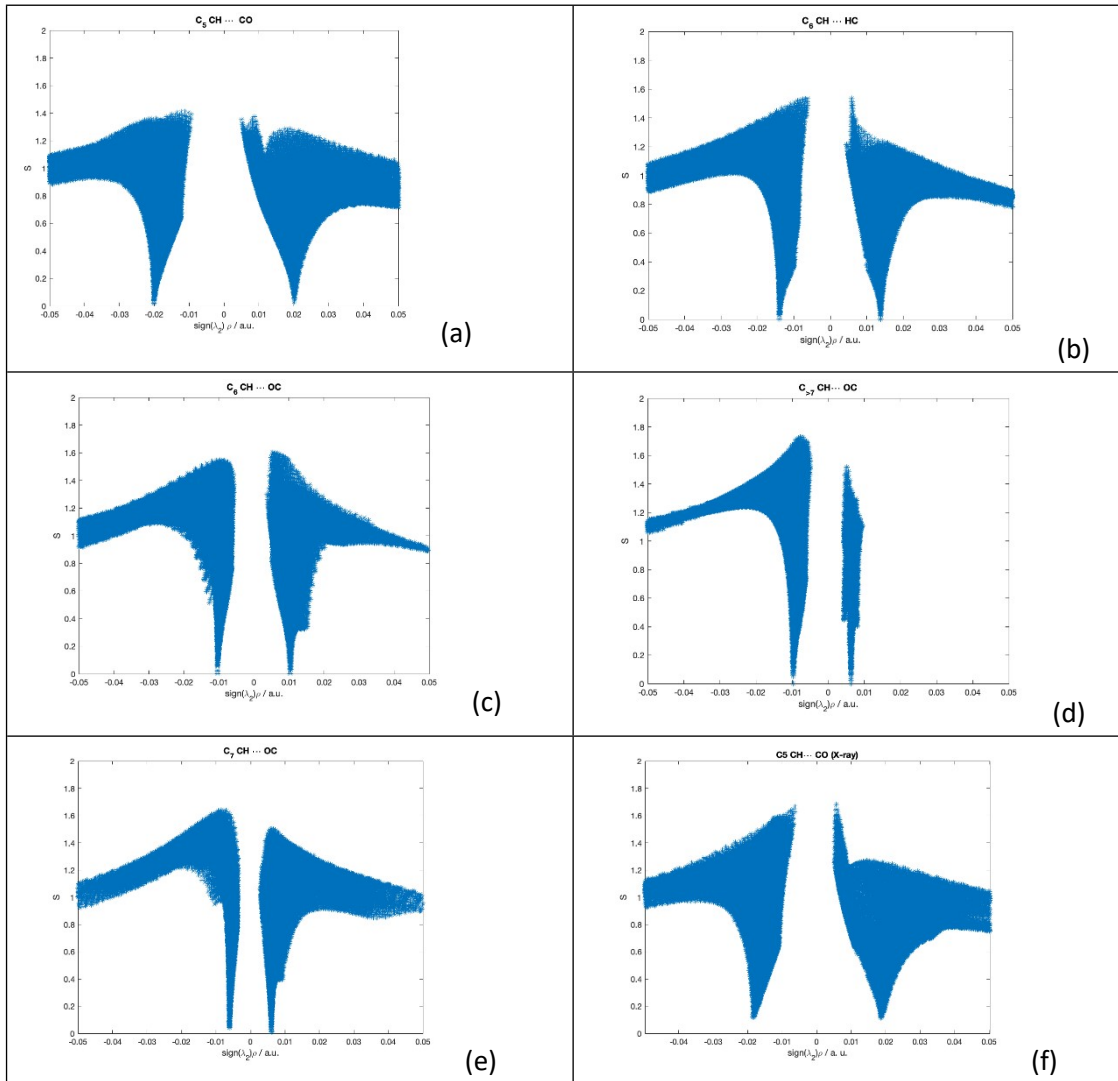


Figure S13. Plot of the reduced density gradient s vs $\text{sign}(\lambda_2)\rho$ for the reference interactions discussed in the text. BCPs (RCPs) correspond to points with $s = 0$ on the negative (positive) side of the abscissa. These points are missing in subplots a, e and f. Subplots a-e refer to the B3LYP-6-311+G(d,p)//B3LYP-6-311+G(d,p) calculation, subplot f refers to the B3LYP-6-311G(d,p)//X-ray calculation.

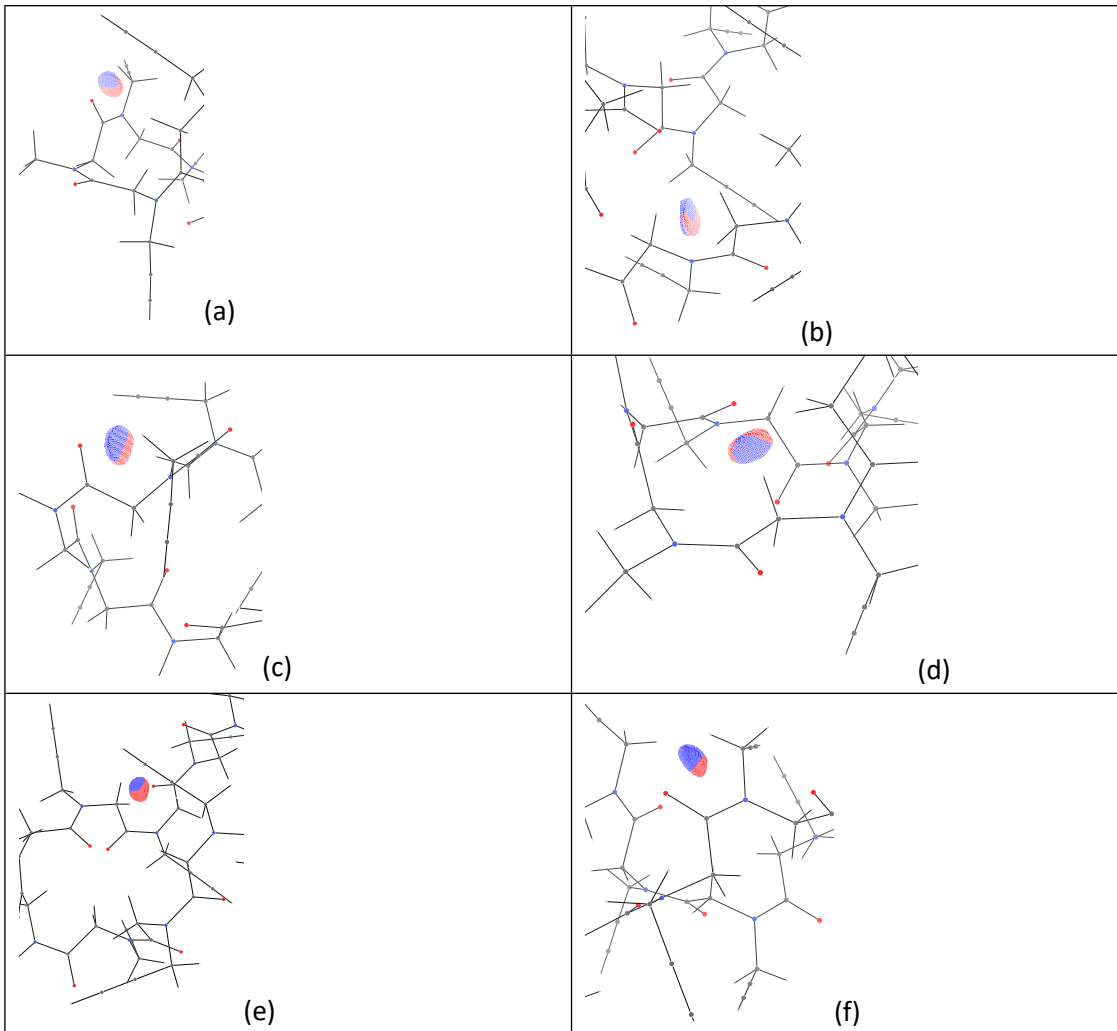


Figure S14. Points with value of the reduced density gradient s in the interval [0.06,0.07] colored according to the sign of λ_2 for the same interactions of Fig. S9: Red and blue points indicate negative and positive values of λ_2 , corresponding to repulsive and attractive interactions, respectively.

6.3 Cartesian coordinates of fully optimized 1 at the B3LYP/6-311G(d,p) level

O	-3.51661300	1.13155900	-0.61404100
O	-2.76815200	0.98402800	2.54275300
O	-0.51010100	-2.74507300	-3.48986200
N	-3.76560800	-2.76581500	1.08026200
O	-6.46886500	-3.25507300	0.90865400
O	-6.94375000	-0.12241300	-1.67945700
O	-2.24172000	-3.99423300	-0.08453600
N	0.54255700	-0.59182600	-2.23653500
N	-2.52663300	-2.67752500	-2.42991300
N	-2.98523700	2.90622100	0.68787000
N	-7.07676900	-1.05899500	0.87202000
N	-6.05433500	1.90535300	-1.15161100
C	-3.85002700	2.17485500	-0.06078100
C	-1.71305700	1.25425700	1.98888300
C	-3.05333400	-3.07996300	-0.04219900
C	-4.69259400	-1.65181000	1.15210500
H	-4.39461200	-0.88492100	0.44258000
H	-4.59405400	-1.18939400	2.13977000
C	-6.15714500	-2.07704400	0.94604900
C	-1.25094400	-2.25250500	-2.65059800
C	-3.33194100	-2.23318700	-1.30638900
H	-4.38536300	-2.33028000	-1.58452800
H	-3.17146600	-1.17265400	-1.12076600
C	-6.70531900	0.32814400	0.66813000
H	-5.79997800	0.55808400	1.22582900
H	-7.49474800	0.95935900	1.09018200
C	0.52461300	0.36322400	-3.35549800
H	1.56003400	0.51064100	-3.66317000
H	-0.01518900	-0.08086000	-4.19978600
C	-5.29232100	2.70673900	-0.21525400
H	-5.78768400	2.73169700	0.75679900
H	-5.27810500	3.73911400	-0.57369700
C	-1.65854200	2.35572000	0.91123300
H	-0.98860800	3.15981000	1.21741100
H	-1.28465500	1.94629100	-0.02720300
C	-6.55939300	0.66740100	-0.83460600
C	-3.71283500	-3.70477100	2.21505200
H	-4.63716800	-4.29079100	2.21991900
H	-2.87858800	-4.37848900	2.01889700
C	-0.06966900	1.64745500	-2.98896100
C	-0.74871200	-1.07707900	-1.77981700
H	-1.45066200	-0.24129600	-1.80802400
H	-0.69519700	-1.39389600	-0.73671700
C	-3.38495300	4.06842400	1.49334900
H	-4.40294100	3.93814700	1.86630600
H	-2.74911200	4.08594700	2.38136100
C	-8.48720100	-1.41902300	0.66092300
H	-8.77243300	-1.16875600	-0.36525400
H	-8.54743300	-2.50279200	0.76705100

C	-9.37906600	-0.75838200	1.61338900
C	-2.99130300	-3.87196500	-3.15364200
H	-2.21199200	-4.12320900	-3.87330500
H	-3.07395700	-4.70355600	-2.44627300
C	-3.27350800	5.34018300	0.77434200
C	-3.54830200	-3.05150800	3.51120400
C	-0.55149500	2.71080600	-2.70458300
H	-0.95694100	3.66048700	-2.45321200
C	-5.86084300	2.20842400	-2.57929200
H	-4.79950800	2.10784300	-2.83425000
H	-6.40057900	1.44172000	-3.13551200
C	-10.12012900	-0.20281500	2.37867100
H	-10.78085600	0.27094200	3.06269800
C	-3.45987600	-2.54664000	4.59783400
H	-3.37517900	-2.10358300	5.55980300
C	-3.18735800	6.38146200	0.18293900
H	-3.10213100	7.30555800	-0.33526700
C	-6.34259700	3.54119800	-2.93637300
C	-6.72035000	4.64121200	-3.23606800
H	-7.06707200	5.60764500	-3.50966500
C	-4.26750800	-3.65042000	-3.83088200
C	-5.32733100	-3.47309700	-4.36681300
H	-6.26502700	-3.31305600	-4.83996900
O	3.51661300	-1.13155900	0.61404100
O	2.76815200	-0.98402800	-2.54275300
O	0.51010100	2.74507300	3.48986200
N	3.76560800	2.76581500	-1.08026200
O	6.46886500	3.25507300	-0.90865400
O	6.94375000	0.12241300	1.67945700
O	2.24172000	3.99423300	0.08453600
N	-0.54255700	0.59182600	2.23653500
N	2.52663300	2.67752500	2.42991300
N	2.98523700	-2.90622100	-0.68787000
N	7.07676900	1.05899500	-0.87202000
N	6.05433500	-1.90535300	1.15161100
C	3.85002700	-2.17485500	0.06078100
C	1.71305700	-1.25425700	-1.98888300
C	3.05333400	3.07996300	0.04219900
C	4.69259400	1.65181000	-1.15210500
H	4.39461200	0.88492100	-0.44258000
H	4.59405400	1.18939400	-2.13977000
C	6.15714500	2.07704400	-0.94604900
C	1.25094400	2.25250500	2.65059800
C	3.33194100	2.23318700	1.30638900
H	4.38536300	2.33028000	1.58452800
H	3.17146600	1.17265400	1.12076600
C	6.70531900	-0.32814400	-0.66813000
H	5.79997800	-0.55808400	-1.22582900
H	7.49474800	-0.95935900	-1.09018200
C	-0.52461300	-0.36322400	3.35549800
H	-1.56003400	-0.51064100	3.66317000

H	0.01518900	0.08086000	4.19978600
C	5.29232100	-2.70673900	0.21525400
H	5.78768400	-2.73169700	-0.75679900
H	5.27810500	-3.73911400	0.57369700
C	1.65854200	-2.35572000	-0.91123300
H	0.98860800	-3.15981000	-1.21741100
H	1.28465500	-1.94629100	0.02720300
C	6.55939300	-0.66740100	0.83460600
C	3.71283500	3.70477100	-2.21505200
H	4.63716800	4.29079100	-2.21991900
H	2.87858800	4.37848900	-2.01889700
C	0.06966900	-1.64745500	2.98896100
C	0.74871200	1.07707900	1.77981700
H	1.45066200	0.24129600	1.80802400
H	0.69519700	1.39389600	0.73671700
C	3.38495300	-4.06842400	-1.49334900
H	4.40294100	-3.93814700	-1.86630600
H	2.74911200	-4.08594700	-2.38136100
C	8.48720100	1.41902300	-0.66092300
H	8.77243300	1.16875600	0.36525400
H	8.54743300	2.50279200	-0.76705100
C	9.37906600	0.75838200	-1.61338900
C	2.99130300	3.87196500	3.15364200
H	2.21199200	4.12320900	3.87330500
H	3.07395700	4.70355600	2.44627300
C	3.27350800	-5.34018300	-0.77434200
C	3.54830200	3.05150800	-3.51120400
C	0.55149500	-2.71080600	2.70458300
H	0.95694100	-3.66048700	2.45321200
C	5.86084300	-2.20842400	2.57929200
H	4.79950800	-2.10784300	2.83425000
H	6.40057900	-1.44172000	3.13551200
C	10.12012900	0.20281500	-2.37867100
H	10.78085600	-0.27094200	-3.06269800
C	3.45987600	2.54664000	-4.59783400
H	3.37517900	2.10358300	-5.55980300
C	3.18735800	-6.38146200	-0.18293900
H	3.10213100	-7.30555800	0.33526700
C	6.34259700	-3.54119800	2.93637300
C	6.72035000	-4.64121200	3.23606800
H	7.06707200	-5.60764500	3.50966500
C	4.26750800	3.65042000	3.83088200
C	5.32733100	3.47309700	4.36681300
H	6.26502700	3.31305600	4.83996900

6.4 Cartesian coordinates of fully optimized 1 at the B3LYP/6-311+G(d,p) level

O	-3.56988600	1.12792800	-0.54356400
O	-2.79165100	1.05161700	2.63060500
O	-0.53545500	-2.84755800	-3.51722400
N	-3.77187300	-2.78110900	1.10718200

O	-6.47027400	-3.31190200	0.90033000
O	-6.98672300	-0.13713800	-1.71415200
O	-2.24240700	-4.03497000	-0.02367400
N	0.56505300	-0.68918300	-2.29708400
N	-2.52320400	-2.75976700	-2.40532600
N	-3.06886800	2.93099900	0.72947300
N	-7.10831300	-1.12467000	0.83011500
N	-6.10771900	1.88415200	-1.14403000
C	-3.92056200	2.17739800	-0.01152700
C	-1.74920300	1.32912700	2.05486000
C	-3.05332400	-3.11807300	-0.00462500
C	-4.71771700	-1.68025100	1.14285200
H	-4.42208900	-0.92213900	0.42252800
H	-4.64112200	-1.19944400	2.12363500
C	-6.17519700	-2.12786800	0.92702300
C	-1.24957600	-2.34576200	-2.65931700
C	-3.31483700	-2.28719300	-1.28292700
H	-4.37020700	-2.36673700	-1.55862700
H	-3.13244300	-1.22814900	-1.10710400
C	-6.75616700	0.27064600	0.64320200
H	-5.85552500	0.50474600	1.20593400
H	-7.55539100	0.88537600	1.07140300
C	0.51800000	0.25797500	-3.42259100
H	1.54560300	0.41360500	-3.75173600
H	-0.03271400	-0.19569100	-4.25458600
C	-5.37134800	2.68359700	-0.18447600
H	-5.88134000	2.68236000	0.78029200
H	-5.37463100	3.71981200	-0.53101100
C	-1.72927300	2.41295100	0.95820600
H	-1.07959700	3.23925200	1.25108000
H	-1.34710000	1.99830300	0.02527000
C	-6.60850100	0.63823100	-0.85203300
C	-3.71247800	-3.69201300	2.26609100
H	-4.60774700	-4.32213300	2.26055100
H	-2.84381200	-4.33317300	2.11521000
C	-0.08336600	1.53873600	-3.05516200
C	-0.71417500	-1.17240900	-1.80516500
H	-1.41356600	-0.33388500	-1.81557600
H	-0.63377500	-1.49093800	-0.76441200
C	-3.46802400	4.11044700	1.50875200
H	-4.54706300	4.11007800	1.66229800
H	-3.02683500	4.01952500	2.50554100
C	-8.51439800	-1.50489800	0.62014500
H	-8.79909300	-1.27932000	-0.41205300
H	-8.56802200	-2.58641000	0.74979500
C	-9.41862700	-0.83332900	1.55287500
C	-3.02109000	-3.94805100	-3.11873200
H	-2.25745300	-4.22273500	-3.84646000
H	-3.11611800	-4.77467900	-2.40696200
C	-3.05409600	5.37356900	0.89268600
C	-3.61761300	-2.99942600	3.54821800

C	-0.57051400	2.60150400	-2.77587700
H	-0.98151400	3.55082800	-2.53132500
C	-5.90996200	2.21568000	-2.56555800
H	-4.85316000	2.08958600	-2.82914000
H	-6.47487800	1.48227400	-3.14124800
C	-10.17373800	-0.27347100	2.30253600
H	-10.84640100	0.20556600	2.97150800
C	-3.57876400	-2.46102000	4.62222100
H	-3.54028600	-1.98614000	5.57217800
C	-2.70964500	6.40954700	0.39169900
H	-2.39611400	7.32602800	-0.04654700
C	-6.35035200	3.57075900	-2.88940700
C	-6.69546600	4.68813700	-3.16689700
H	-7.00988800	5.67119500	-3.42086500
C	-4.29931400	-3.70315400	-3.78405400
C	-5.36045800	-3.50762600	-4.31288700
H	-6.29967600	-3.33124800	-4.77776200
O	3.56988600	-1.12792800	0.54356400
O	2.79165100	-1.05161700	-2.63060500
O	0.53545500	2.84755800	3.51722400
N	3.77187300	2.78110900	-1.10718200
O	6.47027400	3.31190200	-0.90033000
O	6.98672300	0.13713800	1.71415200
O	2.24240700	4.03497000	0.02367400
N	-0.56505300	0.68918300	2.29708400
N	2.52320400	2.75976700	2.40532600
N	3.06886800	-2.93099900	-0.72947300
N	7.10831300	1.12467000	-0.83011500
N	6.10771900	-1.88415200	1.14403000
C	3.92056200	-2.17739800	0.01152700
C	1.74920300	-1.32912700	-2.05486000
C	3.05332400	3.11807300	0.00462500
C	4.71771700	1.68025100	-1.14285200
H	4.42208900	0.92213900	-0.42252800
H	4.64112200	1.19944400	-2.12363500
C	6.17519700	2.12786800	-0.92702300
C	1.24957600	2.34576200	2.65931700
C	3.31483700	2.28719300	1.28292700
H	4.37020700	2.36673700	1.55862700
H	3.13244300	1.22814900	1.10710400
C	6.75616700	-0.27064600	-0.64320200
H	5.85552500	-0.50474600	-1.20593400
H	7.55539100	-0.88537600	-1.07140300
C	-0.51800000	-0.25797500	3.42259100
H	-1.54560300	-0.41360500	3.75173600
H	0.03271400	0.19569100	4.25458600
C	5.37134800	-2.68359700	0.18447600
H	5.88134000	-2.68236000	-0.78029200
H	5.37463100	-3.71981200	0.53101100
C	1.72927300	-2.41295100	-0.95820600
H	1.07959700	-3.23925200	-1.25108000

H	1.34710000	-1.99830300	-0.02527000
C	6.60850100	-0.63823100	0.85203300
C	3.71247800	3.69201300	-2.26609100
H	4.60774700	4.32213300	-2.26055100
H	2.84381200	4.33317300	-2.11521000
C	0.08336600	-1.53873600	3.05516200
C	0.71417500	1.17240900	1.80516500
H	1.41356600	0.33388500	1.81557600
H	0.63377500	1.49093800	0.76441200
C	3.46802400	-4.11044700	-1.50875200
H	4.54706300	-4.11007800	-1.66229800
H	3.02683500	-4.01952500	-2.50554100
C	8.51439800	1.50489800	-0.62014500
H	8.79909300	1.27932000	0.41205300
H	8.56802200	2.58641000	-0.74979500
C	9.41862700	0.83332900	-1.55287500
C	3.02109000	3.94805100	3.11873200
H	2.25745300	4.22273500	3.84646000
H	3.11611800	4.77467900	2.40696200
C	3.05409600	-5.37356900	-0.89268600
C	3.61761300	2.99942600	-3.54821800
C	0.57051400	-2.60150400	2.77587700
H	0.98151400	-3.55082800	2.53132500
C	5.90996200	-2.21568000	2.56555800
H	4.85316000	-2.08958600	2.82914000
H	6.47487800	-1.48227400	3.14124800
C	10.17373800	0.27347100	-2.30253600
H	10.84640100	-0.20556600	-2.97150800
C	3.57876400	2.46102000	-4.62222100
H	3.54028600	1.98614000	-5.57217800
C	2.70964500	-6.40954700	-0.39169900
H	2.39611400	-7.32602800	0.04654700
C	6.35035200	-3.57075900	2.88940700
C	6.69546600	-4.68813700	3.16689700
H	7.00988800	-5.67119500	3.42086500
C	4.29931400	3.70315400	3.78405400
C	5.36045800	3.50762600	4.31288700
H	6.29967600	3.33124800	4.77776200

7.0 References

1. Bruker (2015). APEX3, SAINT and SADABS. Bruker AXS Inc, Madison, Wisconsin, USA.
2. G. M. Sheldrick, *Acta Cryst.*, **A64**, 2008, 112–122.
3. G. M. Sheldrick, *Acta Cryst.*, **C71**, 2015, 3–8.
4. O. V. Dolomanov, L. J. Bourhis, R. J. Gildea, J. A. K Howard and H. Puschmann, *J. Appl. Cryst.*, 2009, **42**, 339–341.
5. C. F. Macrae, I. Sovago, S. J. Cottrell, P. T. A. Galek, P. McCabe, E. Pidcock, M. Platings, G. P. Shields, J. S. Stevens, M. Towler and P. A. Wood, *J. Appl. Cryst.*, 2020, **53**, 226–235.
6. R. F. W. Bader, Atoms in Molecules - A Quantum Theory; Oxford University Press, Oxford, 1990.
7. G. Monaco, F. F. Summa and R. Zanasi, *J. Chem. Inf. Model.*, 2021, **61**, 270–283.
8. M. J. Frisch, G. W. Trucks, H. B. Schlegel, G. E. Scuseria, M. A. Robb, J. R. Cheeseman, G. Scalmani, V. Barone, G. A. Petersson, H. Nakatsuji, X. Li, M. Caricato, A. V. Marenich, J. Bloino, B. G. Janesko, R. Gomperts, B. Mennucci, H. P. Hratchian, J. V. Ortiz, A. F. Izmaylov, J. L. Sonnenberg, D. Williams-Young, F. Ding, F. Lipparini, F. Egidi, J. Goings, B. Peng, A. Petrone, T. Henderson, D. Ranasinghe, V. G. Zakrzewski, J. Gao, N. Rega, G. Zheng, W. Liang, M. Hada, M. Ehara, K. Toyota, R. Fukuda, J. Hasegawa, M. Ishida, T. Nakajima, Y. Honda, O. Kitao, H. Nakai, T. Vreven, K. Throssell, J. A. Montgomery, Jr., J. E. Peralta, F. Ogliaro, M. J. Bearpark, J. J. Heyd, E. N. Brothers, K. N. Kudin, V. N. Staroverov, T. A. Keith, R. Kobayashi, J. Normand, K. Raghavachari, A. P. Rendell, J. C. Burant, S. S. Iyengar, J. Tomasi, M. Cossi, J. M. Millam, M. Klene, C. Adamo, R. Cammi, J. W. Ochterski, R. L. Martin, K. Morokuma, O. Farkas, J. B. Foresman and D. J. Fox,. *Gaussian16, Revision C.01*; Gaussian, Inc.: Wallingford CT, 2016.
9. E. Espinosa, E. Molins and C. Lecomte, *Chem. Phys. Lett.*, 1998, **285**, 170–173.
10. A. Romanova, K. Lyssenko and I. Ananyev, *J. Comput. Chem.*, 2018, **39**, 1607–1616.
11. M. Jabłoński and G. Monaco, *J. Chem. Inf. Model.*, 2013, **53**, 1661–1675.